OREGON HEALTH & SCIENCE UNIVERSITY
SCHOOL OF MEDICINE – GRADUATE STUDIES

Influence of Tube Current and Tube Potential on Two CT Manufacturer Platforms: A Preliminary Phantom Study

By
Isaac J. Bailey

A THESIS

Presented to
Oregon Health & Science University
School of Medicine
in partial fulfillment of
the requirements for the degree of

Master of Science

Presented May 25, 2017

OREGON HEALTH & SCIENCE UNIVERSITY
SCHOOL OF MEDICINE – GRADUATE STUDIES

School of Medicine

Oregon Health & Science University

CERTIFICATE OF APPROVAL

This is to certify that the Master's thesis of

Isaac J. Bailey

has been approved

Mentor/Advisor

Member

Member

TABLE OF CONTENTS

LIST OF FIGURES

FIGURE

LIST OF TABLES

TABLE

ACKOWLEDGMENTS

I would first like to acknowledge the faculty and staff of Oregon State University and Oregon Health & Science University for the in-depth education I received that has unquestionably set me up for future success in the field of medical physics.

I would also like to thank the members of my thesis advisory committee that includes Dr. Krystina Tack and Dr. Thomas Griglock. Thank you for all the help and advice, both in the classroom, and with my residency applications and interview process.

Finally, I would like to extend a special thank you to the last member of my thesis advisory committee and my thesis advisor Dr. Lindsay DeWeese. The continuous help, motivation, and input on my thesis and on my future endeavors in medical physics are sincerely appreciated. She consistently provided guidance when I had a question in regards to my thesis or a various other topic in diagnostic imaging.

For all the above mentioned, I am very grateful.

AN ABSTRACT OF THE THESIS OF

Isaac J. Bailey for the degree of Master of Science in Medical Physics presented on May 25, 2017
Title: Influence of Tube Current and Tube Potential on Two CT Manufacturer Platforms: A Preliminary Phantom Study
Abstract Approved:

Lindsay DeWeese

Objective: The purpose of this study is to further the understanding of the influences of tube current and tube potential in CT by analyzing the adjustment of tube potential in combination with tube current modulation on two CT vendor platforms with the use of a uniform water equivalent phantom. Specifically, this study aims to further the understanding of the impacts of changing tube potential and tube current on CT image quality, as well as radiation dose indices.

Methods: A phantom study was conducted on the Toshiba Aquilion ONE ViSION and Philips iCT scanners at Oregon Health & Science University. Three different phantom configurations were scanned on both CT scanners with three different scan set-ups. The three phantom configurations consisted of scanning the ACR CT accreditation phantom (Gammex 464), along with the addition of two different sized water-equivalent attenuating rings placed around the phantom. The AP and LAT dimensions of the three configurations were: 20cm x 20cm (ACR phantom), 25cm x 35cm (small ring and ACR), and 30cm x 38cm (large ring and ACR). The first scan set-up utilized automatic tube current modulation (ATCM) at the kV automatically selected by Toshiba's ^{SURE}kV application, as well the three additional available kVs. Scan settings followed the recommended vendor settings from the AAPM CT protocols for adult abdomen/pelvis CT. Secondly, fixed $CTDI_{Vol}$'s of 10, 15, and 20 mGy were set, corresponding to the three phantom configurations by size. Lastly, each phantom set-up was scanned at a fixed tube current of 300 mA and all available kVs.

Results: With ATCM and ^{SURE}kV implemented, 80 kV was automatically selected for all three phantom configurations. The Toshiba scans with ATCM and ^{SURE}kV implemented displayed an increase in CNR for all phantom configurations (3% to 27%) when compared to the reference protocol at 120 kV. Comparatively, all three phantom configurations on the Philips resulted in lower CNR's at 80 kV (12.7% to 16.1%). Changing tube potential had varied effects on the $CTDI_{Vol}$ for each phantom

configuration for both vendors. The Toshiba scans with a fixed $CTDI_{Vol}$ exhibited decreasing CNR with an increasing tube potential with all configurations. The Philips scans with ATCM demonstrated a constant $CTDI_{Vol}$ with changing kVs for each phantom configuration. For the scans performed at a fixed tube current, the Toshiba $CTDI_{Vol}$ increased by a factor of 3.19 from 80 to 120 kV and by a factor of 3.47 on the Philips.

Conclusion: While the implementation of Toshiba's ^{SURE}kV resulted in varied effects on $CTDI_{Vol}$, an improvement in image quality was evident for all three phantom sizes when used in conjunction with ATCM. Additionally, on the Toshiba CT with a fixed $CTDI_{Vol}$, CNR increased with decreasing tube potential. These results were not evident on the Philips, however the $CTDI_{Vol}$ remained constant with a change in tube potential when ATCM was employed. Overall, this research provides a further understanding of the impacts of tube current and tube potential on uniform water equivalent phantoms in CT.

1. Introduction

Clinically, the role of a medical physicist in diagnostic radiology has an overall focus on benefiting the patient. The first responsibility of the medical physicist is to aid in the implementation of current technology to create the best possible diagnostic quality images. Secondly, ensuring patient safety, which includes radiation, mechanical and electrical safety is part of confirming benefits are maximized while possible detriments to the patient are minimized [1]. These responsibilities are consistent across all imaging modalities, while the radiation safety aspect is further stressed with imaging modalities having higher radiation output. For example, Computed Tomography (CT) is the current largest contributor to medical radiation exposure among the U.S. and European populations, thus bringing with it, a further stress on radiation dose reduction [2]. It is widely accepted that the first aim of CT technology is to create the best diagnostic quality images, while the second aim is to minimize radiation dose to the patient [3]. This accountability is not alone put on the medical physicist, but is a responsibility also shared by the modality technologist, radiologist, and the manufacturer of the equipment.

Currently Computed Tomography systems have several features that aim to maintain and maximize image quality while pursuing the reduction of dose. A common principle of medical physics first introduced in an effort to reduce exposure to radiation workers in ICRP Publication 26, is known as ALARA, “as low as reasonably achievable” [4]. The concepts surrounding ALARA and the reduction of exposure have since been expanded to include patient safety as well. There have been many advancements in CT technology which have sought to reduce and optimize radiation dose. These include automatic tube current modulation (ATCM), bowtie filtration, iterative reconstruction, scanning length reduction, and automatic kV selection. Of those mentioned, ATCM and automatic kV selection are the topics of specific interest for this study.

ATCM techniques allow for adaptations of the tube current in the x-y- and z-plane according to attenuation information derived from the topogram or scout image [5]. These techniques adjust the x-ray tube current while the tube voltage is kept constant (standard tube voltage is 120 kV for adult chest and abdominal studies). The tube current is adjusted over the scan length so the detector is receiving the minimal amount of x-rays necessary to maintain the user specified diagnostic image quality requested. By doing this, there is no surplus of x-rays through areas of anatomy with low attenuation, thus minimizing radiation dose to the patient. Adjusting the tube voltage for maximizing image quality outputs a less penetrating spectrum that is more likely to be attenuated in the anatomy, thus increasing the inherent contrast in tissues. However, if tube voltage is decreased, an increase in image noise is expected because the x-ray beam will be more greatly attenuated and less x-rays will be contributing to image formation.

With the application of ATCM an increase in radiation output could be observed due to the system's compensation for the less penetrating beam. The complexity of adjusting tube potential and current to maintain the best possible diagnostic image quality brought about the development of automatic kV selection. Automatic kV technology adjusts tube current and tube potential in tandem based off of the scout image attenuation information [5]. Siemens was the first manufacturer to release automatic kV selection technology and only Toshiba has since also come out with their automatic kV selection technology. With the relative novelty of such technology, the amount of current research on the implementation of automatic kV selection systems is limited and so is the clinical application of such technology. Toshiba's ^{SURE}kV is advertised to be effective when implemented in CTA studies, but has not seen large-scale implementation with general chest or abdominal studies [6]. Additional research on the functionality of this new tool and the interplay with ATCM algorithms and auto kV will further the understanding of auto kV and enable additional applications of the technology clinically.

The purpose of this thesis is to assess the impact of changing tube potential and tube current modulation on two major CT manufacturer platforms in an effort to further the understanding of the influences on adult abdomen CT exams. Specifically, this research will analyze data from phantom studies on both Toshiba and Philips CT systems to evaluate the impact of changing tube potential on image quality while secondarily analyzing what effect it has on radiation dose indices for the patient. As Toshiba currently has an automatic kV selection tool, examination of the impacts of this tool in conjunction with ATCM will be of additional interest. This study will add to the existing knowledge about tube potential selection techniques with the aim of improving clinical scans in the future. An overview of CT technology will be discussed in upcoming sections of this thesis. This will consist of an in depth look at CT image quality, CT dose indices, ATCM, automatic kV selection, and previous studies on automatic kV selection technology. This thesis will be concluded by stating the methodology of this study, the results, and a discussion of the results. The objective of this thesis is to support a discussion of adjusting tube potential manually or automatically, by understanding the impacts, applications, and possible further implementation of such technology to advance patient care in diagnosis and safety.

2. Background

2.1 Computed Tomography (CT)

The first CT scanner was developed by Sir Godfrey N. Hounsfield and was first being used clinically in 1973 [7]. Initially, these scans took many hours for the acquisition and processing of the image data. Originally, CT was known as computed axial tomography (CAT) due to the formation of axial images of the anatomy. The continuous development of these systems has brought with it the capabilities to have three-dimensional image data sets which include axial, coronal, and sagittal images. This ultimately changed the name of such technology to simply computed tomography (CT) [8].

Reduction in image acquisition time, increased computing power, and improvement in image quality have caused vast growth in the CT clinical environment in the last 30 years.

CT technology uses similar principles employed in conventional x-ray imaging, but instead of a fixed x-ray tube, CT uses an x-ray tube capable of rotating around the patient in a circular structure known as the gantry. During a CT scan, the patient lies on a table that slowly moves through the gantry while the x-ray tube rotates around the patient projecting an x-ray beam through the patient's anatomy. CT scanners use digital x-ray detectors located opposite the x-ray source as represented in Figure 1.

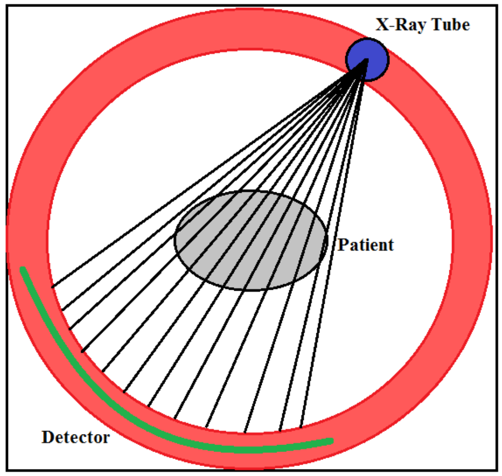

Figure 1: CT fan beam projection

With each rotation of the x-ray tube around the patient, tomographic or cross sectional images are generated by the CT system [9]. After the completion of a CT scan, the cross-sectional slices are 'stacked' to create the three dimensional image set of the patient which can then be oriented in the requested viewing plane.

CT technology takes advantage of the fact that soft tissue is primarily made of carbon, hydrogen, oxygen, and nitrogen and each have their own specific linear attenuation coefficient making them distinguishable based off the attenuation information obtained in the CT scan [8]. The linear attenuation coefficient value indicates the fraction of photons interacting per unit thickness of material. This fraction is dependent on the energy of the photons and atomic number and density of the material [10].

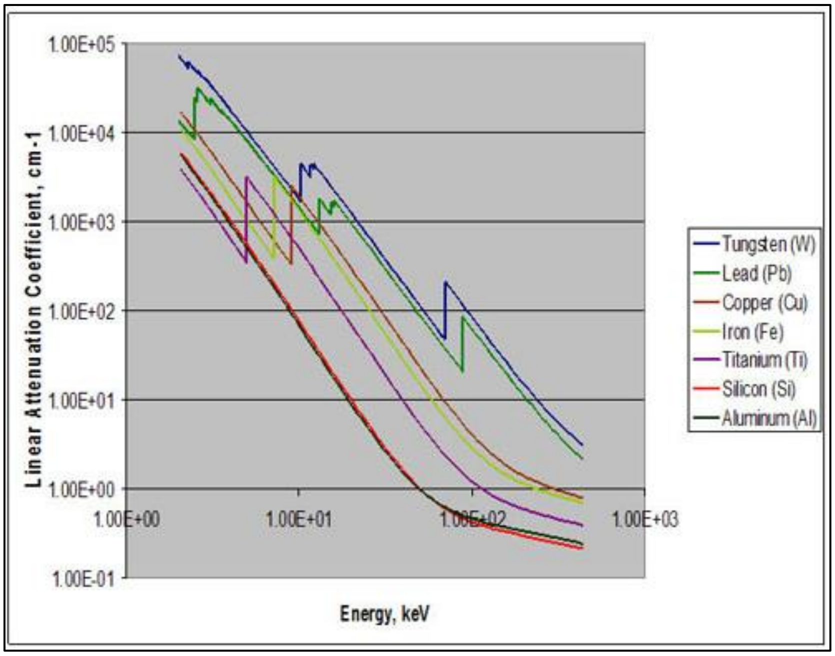

Figure 2: Linear Attenuation Coefficient Changing with material and Energy [11]

Each voxel in a CT image is assigned a value called a CT number. The CT number is representative of the gray scale value of the voxel, which correlates to important information known as Hounsfield units (HUs), in reference to Sir Godfrey Hounsfield. The Hounsfield unit by definition is:

$$\text{HU or } CT\ Number = 1000\,\frac{\mu(object)-\mu(water)}{\mu(water)} \qquad (1)$$

In equation 1, μ(object) is the linear attenuation coefficient for the object or tissue the x-ray beam is being projected through and μ(water) is the linear attenuation coefficient for water. Because of this relationship, the four basic materials of interest have HU values as follows at 120 kV: Water = 0, Fat = -60 to -120, Air = -1000, and Compact Bone = +1000 [12]. These values change with kV as the linear attenuation coefficient is energy dependent as shown in Figure 2. CT image data helps to represent the specific tissue makeup in the region of interest.

Due to the information obtained in a CT scan, there exists a wide array of uses clinically. It has grown into a useful screening tool for identifying disease, in the form of either tumors or lesions due to its ability to provide tissue information which aides in detecting irregular anatomical densities in various regions of interest. In the specialty of neuroradiology, a CT scan is often used to detect several ailments or injuries including tumors, clots, and hemorrhages in the head [9]. Additionally, a CT scan is specifically useful in musculoskeletal radiology for imaging bone fractures and bone tumors due to the high contrast boundaries between the bony anatomy and the surrounding soft tissue.

2.1.1. CT Image Quality

As mentioned previously, CT scanner technology has been rapidly advancing since its development in the early 1970's. The aim of such medical technology is to benefit the patient to the greatest extent possible. With CT technology, the first goal is to create the best clinical images where the diagnostic accuracy of the scans is dependent on various image quality metrics. It is important that the physicist, physician and technologist understand image quality metrics in CT and what they are dependent on so the image quality can be maximized for the specific anatomical region of interest in the study [13].

The level of image quality represents the accuracy of the representation of the object/anatomy that is perceived by the viewer [13]. Determining image quality requires quantitative measures of image quality that include spatial resolution, CT number accuracy, and low contrast resolution (contrast-to-noise ratio).

Spatial resolution in a sense represents the amount of blur in an image and is a measure of an imaging systems ability to resolve small objects in close proximity to one another. In practice, a pattern consisting of what are called “line pairs” is used to quantitatively measure spatial resolution of an imaging system as shown in Figure 3.

Figure 3: Module 4 of ACR CT Accreditation Phantom

The spatial resolution is termed spatial frequency when denoting the line pairs per centimeter visible. There are numerous factors that influence spatial resolution including focal spot size, magnification, reconstructed slice thickness, reconstruction filter, pixel size, pitch, and patient motion [13].

Low contrast resolution refers to the system’s ability to discern small differences in object density compared to the surrounding anatomy. This is an image quality aspect that makes CT a very useful diagnostic tool compared to that of general radiography.

Low contrast resolution is impacted by the number of x-ray photons interacting, being detected, and contributing to image formation. As the number of x-rays increase, so does the low contrast resolution. An increase in the number of photons contributing to the image can be due to an increase in the tube current, increase in tube potential, increase in image slice thickness, and increase in pixel size. Tube current and tube potential impact the number of photons produced in the x-ray tube, thus the number of x-rays projected through the anatomy to the image detector. Increasing the slice thickness and pixel size influence the number of photons "captured" within each slice or pixel, increasing the low contrast resolution. However, a tradeoff to be considered is that as the number of x-rays produced increases, the radiation dose to the patient also increases. The dose aspect of CT will be discussed in the next section.

Quantum noise 'σ' or often called just noise, is directly dependent of the number of x-rays contributing to image formation. If a diagnostic image has N number of x-ray photons contributing to an image, then the noise for that image is simply $\sigma = \sqrt{N}$. Equation 2 shows how the noise is computed using the means square method and is dependent on the Hounsfield Unit values [8].

$$\sigma = \sqrt{\frac{\sum_{i=1}^{N}(HU_i - \overline{HU})^2}{N-1}} \qquad (2)$$

The contrast-to-noise ratio or CNR is also a very useful and common metric for analyzing CT image quality. CNR takes into consideration both the aspects of noise, which can degrade an image, and contrast which is inherent to the anatomy/tissue. The contrast can be better represented in an image by selecting a tube potential that creates x-ray photons at the necessary energy which maximize differences in the attenuation coefficients for the tissues of interest. Clinically, noise in an image impairs the ability of physicians to resolve small differences in tissue density, which is important when trying to distinguish disease from normal tissue. CNR is defined as:

$$CNR = \frac{|A-B|}{SD_B} \qquad (3)$$

'A' is the mean HU / CT number in the defined structure in the region of interest, 'B' is the mean HU/CT number in the image background outside the ROI, and 'SD_B' is the standard deviation (noise) of the signal in 'B'. The tube current which dictates the number of x-rays produced in the x-ray tube and the tube potential/voltage which impacts the energy and amount of the x-rays will be discussed in sections 3 and 4 respectively.

2.1.2. Radiation Dose in CT

Computed tomography is currently the largest contributor to medical radiation exposure to the U.S. population, and because of this radiation dose in CT is a topic of high importance [2]. There is significant concern and debate about the potential radiation hazards from the radiation levels delivered in a diagnostic CT.   With this concern, a concept has been developed called, "Image Wisely" which promotes radiation safety in adult medical imaging. "Image Gently" was developed for promoting safety in pediatric imaging [14]. These joint campaigns between the ACR, RSNA, AAPM, and ASRT advocate that the benefits of CT outweigh the risks of ionizing radiation, but the goal is to bring awareness to the optimization of scans by obtaining the best image quality with the lowest possible radiation dose [14].

Biological effects of concern with radiation can be broken into two main categories, stochastic effects and deterministic effects. Stochastic or probabilistic effects are of primary concern in CT in relation to the possibility of long term cancer risks. As mentioned above, the benefits of CT exceed the minimal risks, but because the risks are not completely understood, continuous efforts such as Image Wisely are employed in an effort to further reduce dose to patients.

While discussing radiation dose in computed tomography, it is essential to understand the units of CT dose and what they are. The fundamental unit of radiation dose in CT is the Computed Tomography Dose Index (CTDI).

The CTDI characterizes the average absorbed radiation dose along the longitudinal axis (z-axis) from a serious of contiguous CT exposures (slices). It is measured with a pencil ionization chamber which is 100 millimeters in length (thus usually referred to as $CTDI_{100}$). For the measurement of $CTDI_{100}$, the pencil ion chamber is inserted into the center or peripheral holes of a polymethylmethacrylate (PMMA) phantom of 16 or 32 centimeter in diameter. Depending on the vendor, the 32 cm phantom represents the adult torso, while the 16 cm phantom represents an adult head. For pediatrics, the 32 or 16 cm phantom signifies the torso while the 16cm phantom denotes a pediatric head [15].

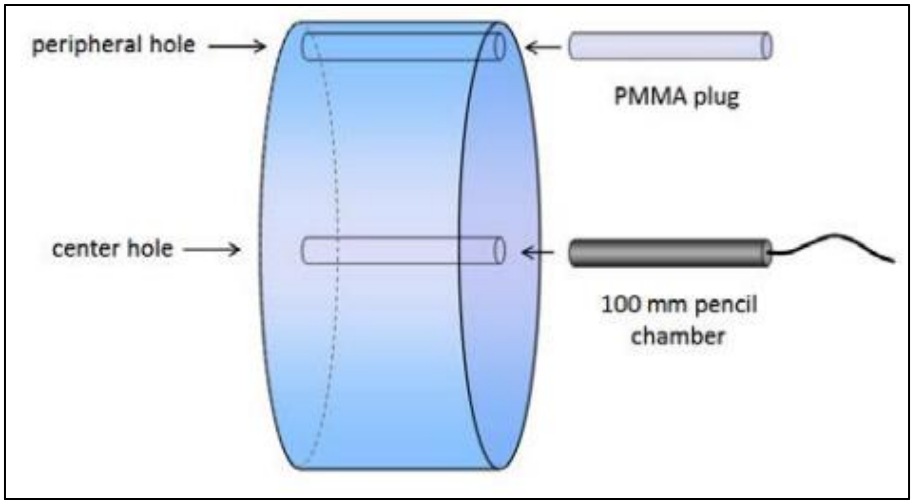

Figure 4: PMMA Phantom used to measure CTDI 100 [14]

The $CTDI_{100}$ is defined as:

$$CTDI_{100} = \frac{1}{nT}\int_{L=-50\,mm}^{+50\,mm} D(z)dz \qquad (4)$$

In the above equation, ‘nT’ represents the nominal x-ray beam width, where ‘n’ is the number of slices per scan and ‘T’ is the slice thickness. D(z) is the measured dose at point z. As mentioned, the $CTDI_{100}$ is measured at the center and peripheral locations of the PMMA phantoms, which aids in estimating the average dose to the phantom, or the weighted CTDI ($CTDI_W$).

When talking about the CTDI it is also important to note that it was never intended as a direct method for patient dose assessment. Technological advancements in CT have required necessary adjustments to the CTDI in an attempt to have greater standardization of CT dosimetry metrics. The deviations of this CTDI are more commonly in use and readily available [16]. These dose indices include $CTDI_W$, $CTDI_{Vol}$, DLP, and SSDE.

The $CTDI_W$ is defined as:

$$CTDI_W = \left(\frac{1}{3}\right) CTDI_{100,Center} + \left(\frac{2}{3}\right) CTDI_{100,Periphery} \qquad (5)$$

In an effort to more accurately represent the dose for clinical CT scan, given the introduction of helical scanning, $CTDI_{Vol}$ was developed. Helical scans are characterized by a specific gap or overlap, known as the pitch, between rotational slices of the x-ray tube, and $CTDI_{Vol}$ took this into consideration. The $CTDI_{Vol}$ is simply the ratio of the $CTDI_W$ to the pitch ($CTDI_W$/Pitch). Pitch is defined as the ratio of table movement distance per gantry rotation, divided by the nominal beam width (nT). $CTDI_{Vol}$ is the most accessible dose indicator and is often displayed on the scanner console prior to the actual scan [16]. $CTDI_{Vol}$ will be the same for CT scans no matter what the scan length so the Dose Length Product (DLP) was established to represent the total amount of radiation delivered or integral dose to the patient. DLP is defined as the scan length multiplied by the $CTDI_{Vol}$ giving it units of mGy-cm [16].

When examining the CT dose indices it is important to remember that these values are exactly that, dose indices. Estimates of individual patient dose must use a size-specific dose estimated as discussed by McCollough, et al. in, “CT Dose Index and Patient Dose: They Are Not the Same Thing” [17]. These dose indices are there to enable medical physicist to compare quantitative values between different CT scanners and between various CT protocols.

To adjust the readily available $CTDI_{Vol}$ to a specific patient size, the SSDE or Size-Specific Dose Estimates was developed to account for the spectrum of patient sizes [16].

SSDE uses the patient's effective diameter ($\sqrt{AP\ x\ LAT} dimensions$), which correlates the patients AP and LAT dimensions to a circle of equal area as represented in Figure 5.

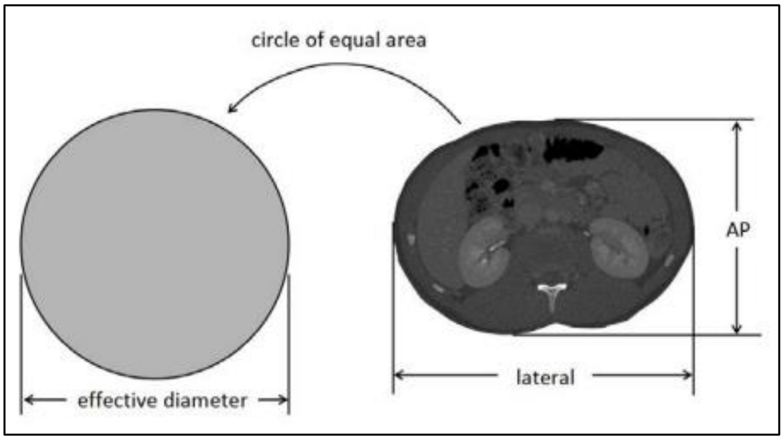

Figure 5: AAPM TG 204 Effective Diameter [14]

The Report of AAPM Task Group 204 has corresponding conversion factors as a function of the effective diameter of the patient and these factors ($f_{size}^{32}\ or\ f_{size}^{16}$ from equations 6 & 7) are used to calculate the SSDE in combination with the $CTDI_{Vol}$. The patient size-specific factor is multiplied by the readilyavailable $CTDI_{Vol}$ to get the SSDE for a given patient as shown in equations 6 and 7 below.

$$SSDE = f_{size}^{32}\ x\ CTDI_{Vol}^{32} \qquad (6)$$

$$SSDE = f_{size}^{16}\ x\ CTDI_{Vol}^{16} \qquad (7)$$

With this equation, the $CTDI_{Vol}$ from the 16 or 32 cm phantom is scaled to account for the specific patient size in an effort to get a better estimate of dose. The Report of AAPM Task Group 204 discusses SSDE as a tool for CT technologists to use by utilizing the displayed $CTDI_{Vol}$ and the available look up tables to estimate the size-specific dose for that scan [14].

2.2 Automatic Tube Current Modulation

Automatic tube current modulation (ATCM) was developed with the same intentions as computed tomography. The first objective of ATCM is to assure diagnostic quality images and the second is to ensure radiation savings to the patient wherever possible. ATCM works in the same fashion as automatic exposure control in general radiography and has now become one of the most prominent and frequently used features on modern CT systems. In short, the CT system's tube current is adjusted automatically during a scan to account for patient attenuation differences due to the varying thickness, shape, and density of anatomy. The tube current is adjusted in the z-axis of the patient (from head to toe) and in the axial plane (x and y axis) [13]. Figure 6 demonstrates longitudinal modulation (z-axis), showing an example of how a lower amount of tube current is needed in the lungs (low density) compared to the bony and higher density region of the pelvis. Figure 6 also demonstrates the modulation in the x-y plane (axial) around the patient based off patient shape and density. Typically, patients have a larger lateral dimension compared to their anteroposterior dimension, resulting in a higher tube current laterally compared to the AP direction.

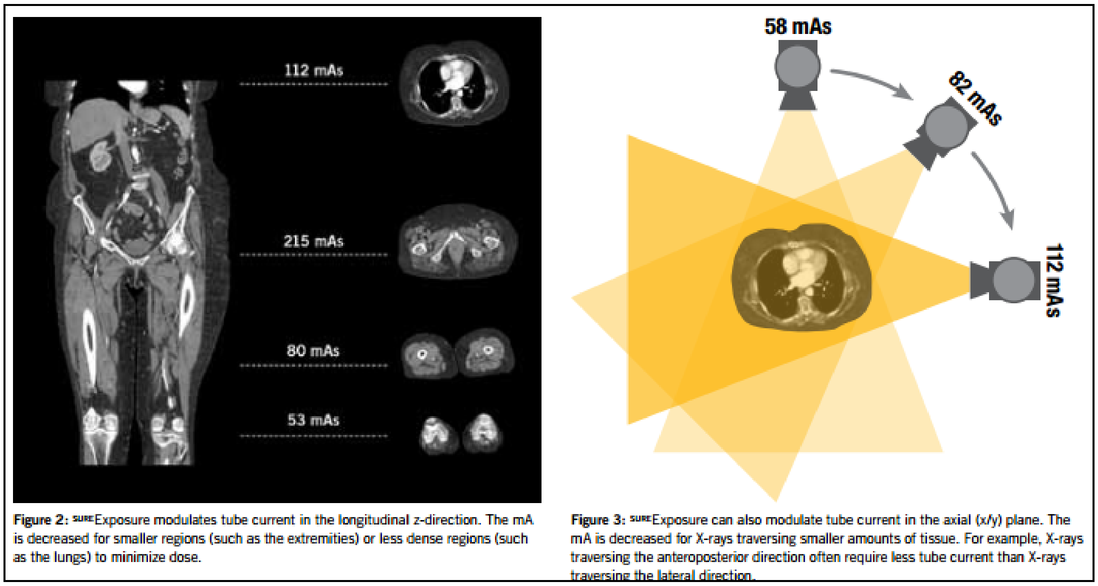

Figure 6: LEFT: Z- Axis Modulation RIGHT: Axial Plane Modulation [3]

To understand the functionality of ATCM, the impacts of changing tube current on image quality and radiation dose need to be understood first. For discussion of tube current it will be assumed that the tube potential and time during which x-rays are being produced are kept constant along with the many other CT techniques and settings. The tube current (mA) directly influences the number of x-rays produced within the x-ray tube by controlling the current in the cathode filament and thus the amount of thermionic emission [18]. Adjusting the tube current will linearly adjust the number of x-ray photons, and in turn the radiation output delivered to the image detector through the patient.

For example, if the tube current is doubled, keeping other parameters constant, the number of x-rays produced in the x-ray tube will be doubled. If the tube current is increased, the radiation dose to the patient will also increase, however this could lead to an improvement in image quality. The more x-ray photons being produced in the x-ray tube can lead to more photons being detected and improving the contrast resolution by reducing the noise in an image. As mentioned previously, the decrease in visible noise with an increase in mA comes at the cost of increasing the radiation exposure to the patient.

ATCM was developed to automate and optimize the impact of tube current on image quality and dose savings in CT as discussed above. Simply put, ATCM adapts the tube current for the varying densities, thicknesses, and shapes of anatomy based off of the attenuation information obtained from scout image(s). The technology is aiming to maintain image quality while reducing dose where less attenuating anatomy allows for it. In addition, a minimum and maximum value of tube current can be set by the user for further dose savings. Because of how it is implemented, ATCM has three important advantages. First, ATCM allows for consistent image quality across patients while secondly, it reduces photon starvation artifacts which aids to the first advantage (image quality). The third advantage is the radiation dose reduction by setting the noise threshold at the highest level possible that does not interfere with the diagnostic quality of the images [13].

These advantages are shown in Figure 7, displaying an example of ATCM adjusting the tube current over the z axis of the scan. If a fixed tube current was utilized for the entire length, it would result in photon starvation in the shoulders and pelvic regions. Additionally, the lungs would be receiving a higher flux of x-ray photons than necessary to match the requested image quality, as they are mostly air and have a very low density. The ATCM reduces the mA in the lung region to maintain image quality and allow for dose savings.

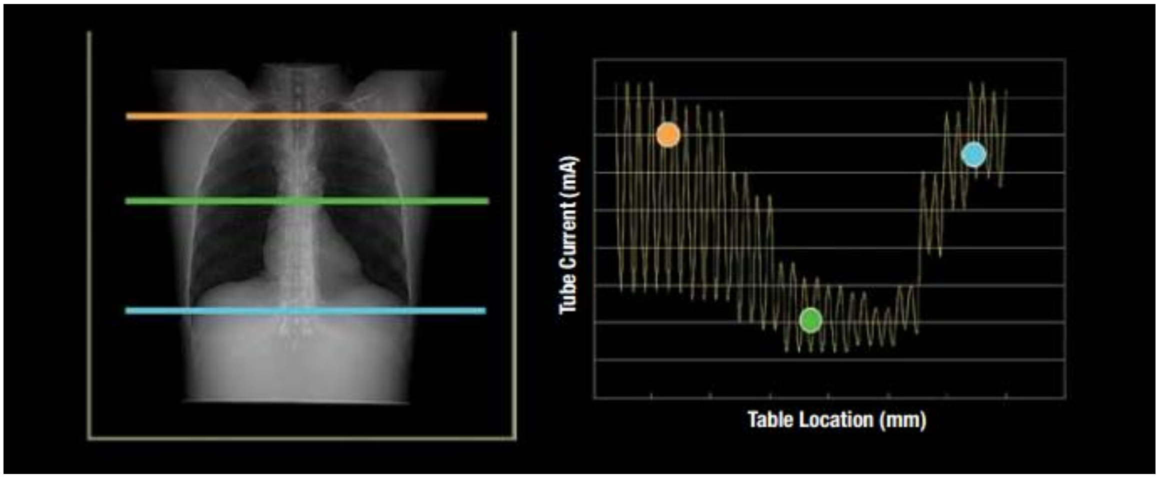

Figure 71: ATCM adjusting tube current over z axis of scan [3]

As the focus of this study is on automatic kV selection and as this function works simultaneously with the ATCM of the system, it is essential to understand ATCM in depth. Each manufacturer or vendor implements their own ATCM in a different way so it is important for the imaging physicist to understand the complexities of ATCM technology and what effect it might have on image quality.

The goal of General Electric's (GE) ATCM system is to keep a constant image noise regardless of attenuation values, with a minimum and maximum tube current value set. The image quality reference parameter GE uses is called the "Noise Index" [19].

The objective of Philips ATCM is to optimize image quality and radiation dose across patients of all sizes through their iPatient platform using their DoseRight CS algorithm. Using the attenuation information from the scout image, the system determines the water equivalent diameter of the patient. Then, based off of the difference between the patient diameter and the reference patient diameter and their image quality parameter called the "Dose Right Index" (DRI), the tube current is then adjusted to obtain the respective mAs/slice for the water equivalent diameter of the patient [20]. Figure 8 shows the optimization of tube current and how it compares to a system with constant noise over varying patient sizes. An increase in DRI by one would decrease image noise by 6% and increase the $CTDI_{Vol}$ by 12%. A decrease in DRI by one results in an increase in noise 6% and a decrease in $CTDI_{Vol}$ 12% [20].

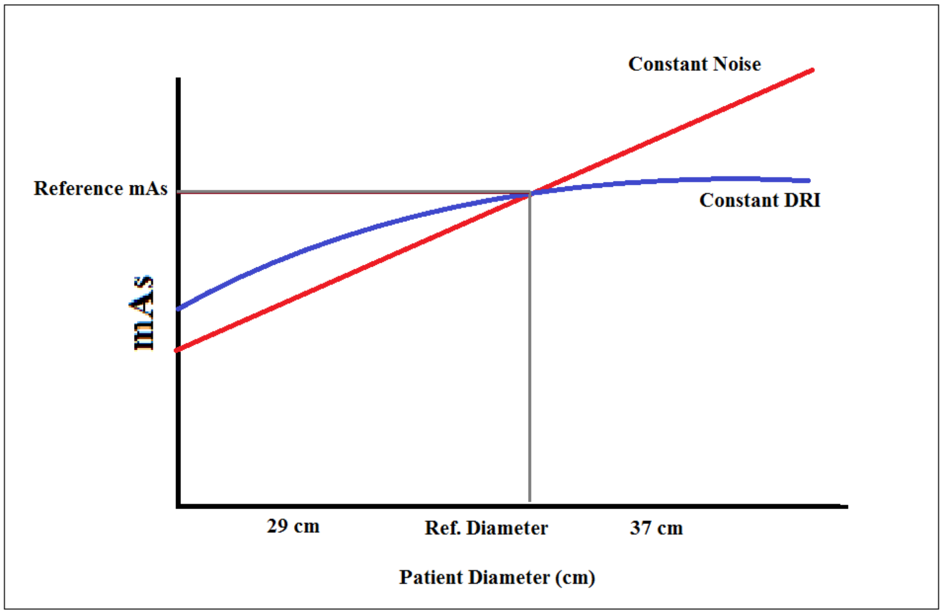

Figure 82: DoseRight Dose Curve

Siemens' ATCM is implemented similarly to Philips' ATCM. Siemens ATCM function is called, "CARE Dose4D" and this function has a user specified reference value for image quality called, "Quality Reference mAs" (QRM). This QRM is expressed in terms of the effective mAs that produces the desired image quality on a standard sized reference patient. The system determines the tube current based on the scout image's attenuation information and then modulates in real time (time being the fourth dimension

4D), to maintain constant image quality over the entire scan range. Siemens claims that with implementation of CARE Dose4D a dose savings of up to 68% can be possible [21].

Toshiba's ATCM is SUREExposure 3D and is similar to GE in that, the goal is to maintain constant image noise regardless of attenuation values and the user can set a minimum and maximum tube current as shown in Figure 9.

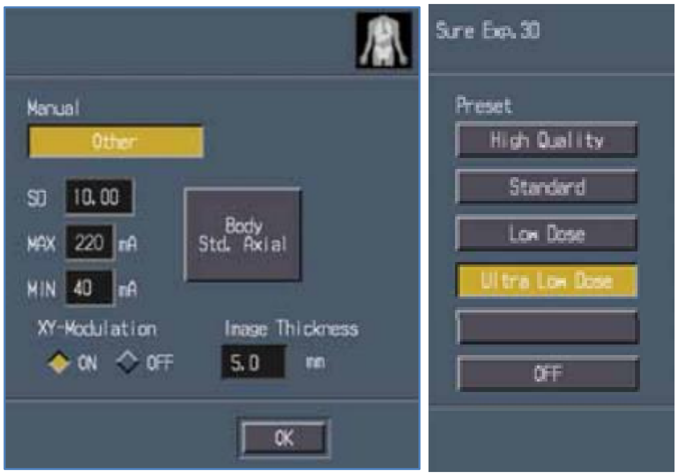

Figure 9: Toshiba SUREExposure 3D interface [3]

Figure 9 also shows that with Toshiba's interface, the user can specify the "Target image quality level" which can be high quality to ultra-low dose. The target image quality level alters the standard deviation (SD) value of the signal in an image with a corresponding slice thickness as shown in Figure 9. Once the user specifies either the SD quantity itself or selects one of the presets, the system will automatically adapt the tube current along the z axis and the x-y plane (axial) to account for attenuation difference information obtained from the dual scout images. Toshiba claims a dose reduction of up to 40 % depending on the individual patient and anatomy being scanned [3].

The difference in the methods of ATCM between Toshiba (constant noise) and Siemens and Philips (constant QRM/DRI) is illustrated in Figure 10. The constant image noise line could represent the functionality of the ATCM with changing patient size. With a constant image noise set, the relative tube current will change linearly with the relative attenuation of the patient.

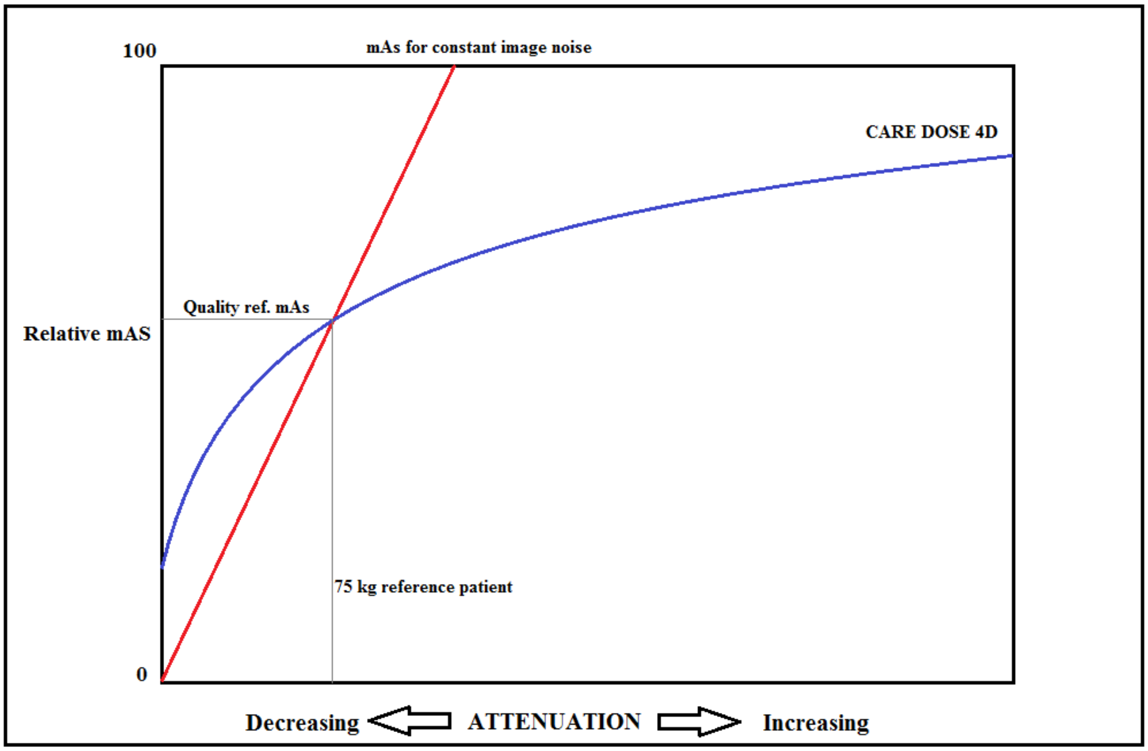

Figure 30: CARE Dose4D Dose Curve

With a system such as Siemens CARE Dose4D and Philips DoseRight, the relative tube current does not change linearly with relative attenuation of the patient. For patients below the reference patient size, relative tube current is decreased, but is greater comparatively to the constant image noise method. Also, the tube output is greater, and noise is lower in comparison to the constant image noise curve with a small reference patient. If the patient is larger than the reference patient, the constant QRM method will result in a lower tube current, lower dose, and higher noise compared to employing a constant noise model. The reason for this is because patients larger than the reference patient generally have more body fat, which increases tissue contrast. Smaller than reference patients will require less dose, but they have less fat and thus less tissue contrast, which requires a slightly higher mAs and resultant dose than would be used with a constant image noise system [22].

2.3 Automatic kV Selection

Automatic kV or tube potential selection was developed in an effort to optimize the impacts of changing the tube potential on the image quality and the possible dose reduction to the patient.

The tube potential or voltage determines the energy of the electrons in the electron beam bombarding the anode within the x-ray tube (100 kV results in electrons of 100 keV in energy) [18]. The average filtered x-ray beam energy is known to be about one third to one half of the maximum electron energy. In computed tomography there is added filtration such as a bow tie filter which ‘hardens’ the beam (filters out low energy x-rays) making the average filtered x-ray beam energy closer to one half the E_{max}. As the x-ray beam energy changes so does the penetrability of the beam. Increasing the tube potential or voltage will increase the average x-ray photon energy as well as the radiation output.

The change of x-ray tube intensity output based on the change in the potential is represented as follows:

$$\text{Change in x-ray beam intensity} \propto \left(\frac{kVpB}{kVpA}\right)^2 \qquad (8)$$

For example, if the kV increases from 80 to 100 you would expect relative output to increase by a factor of $\propto (\frac{100}{80})^2 = 1.56$.

Again, as the x-ray tube potential increases so does the $CTDI_{Vol}$. With the 32 cm PMMA phantom, the $CTDI_{Vol}$ decreases by 68% from 120 kV to 80 kV [13], which is not proportional to: $\propto (\frac{kVB}{kVA})^2$. The increase in $CTDI_{Vol}$ from 80 kV to a higher kV is not proportional to: $\propto (\frac{kVB}{kVA})^2$ because this equation just describes the relative tube output, where $CTDI_{Vol}$ is dependent on other aspects such as filtration, attenuation through a phantom, and scatter from surrounding slices.

While reducing tube potential has been shown to reduce patient radiation exposure, the image quality impact of changing tube potential will be explored. As mentioned, a higher tube potential results in a higher penetrability of the x-ray beam. This leads to less attenuation by the anatomy and a higher flux of x-rays at the image detector, requiring a lower tube current to achieve the same level of image quality. However, because of reduced attenuation by the anatomy, there is less contrast within the image. Lowering the tube potential outputs a less penetrating spectrum that magnifies inherent differences in the attenuation coefficients between tissues, providing greater contrast in the diagnostic image. With the increase in contrast, an increase in noise could result due to more x-ray photons being attenuated and not reaching the image detector. Because ATCM is a prominent function in routine clinical use, it is not certain if lowering tube potential will increase noise or decrease radiation output due to the adaptation of tube current taking place. Depending on the image quality requirements of the ATCM, the decrease in tube potential could require an increase in tube current to maintain the preset image quality level. With this decrease in kV to increase image contrast, image noise is maintained from the ATCM, and radiation output could be increased because of the necessary increase in tube current.

The development of automatic kV selection was brought about by the evolving complexity of adjusting tube current and potential in tandem in order to enhance image quality and reduce radiation dose. Automatic kV selections technology simply adjusts tube current in conjunction with tube potential based off of the scout image attenuation information with the goal of maximizing image quality and optimizing radiation dose.

Siemens' was the first manufacturer to develop an automatic kV selection function and called it, "CARE kV". This system automatically recommends the optimal tube voltage for an individual patient while CARE Dose4D simultaneously adjusts the tube current based off of the anatomy being scanned and the exam protocol. While the QRM was the parameter of interest for the ATCM alone, CNR is the image quality parameter of importance for this system. The aim of this system is to keep the CNR constant with the use of CARE kV. Like with CARE Dose4D, this system uses the attenuation information from the scout image to calculate the mAs necessary for each available tube potential and the user specified level of image quality (CNR). The system then determines the optimal combination of kV and mAs to produce the desired image quality with the lowest patient $CTDI_{Vol}$ [23].

Unlike CARE kV, Toshiba's ^{SURE}kV function does not implement a new image quality metric, rather it will maintain the target image quality level of noise from the

^{SURE}Exposure 3D algorithm. Because of how this technology is implemented, the lowest kV will be selected based off of attenuation information from the scout images, without maxing out the tube current. Toshiba has clinically targeted kV selections of 80, 100, 120, and 135.

Currently both forms of automatic kV technology see implementation mainly in contrast studies such as CT angiography. The reason for this is because there is a high level of image quality improvement evident due to the significant increase in iodine contrast with the reduction in kV. This reduction in kV brings the average x-ray energy closer to the k-edge of iodine, thus a greater attenuation of iodine and a greater difference between the attenuation of the contrast and surrounding tissues [23]. The CNR can be maintained with an increase in image noise, while allowing dose savings to the patient. Less benefit is seen with non-contrast studies as the increase in attenuation of tissue is less evident. These studies also would require higher mAs to reduce image noise, thus not necessarily decreasing patient dose [23].

Where Philips does not currently have auto kV function, they do have techniques built into their iPatient platform that aids in maintaining image quality in contrast exams where a decrease in tube potential is beneficial to increase the contrast between the iodine and surrounding tissue. As stated above, a decrease in tube current with the mAs held constant would decrease the $CTDI_{Vol}$ but increase the image noise. With DoseRight, if the planned tube potential (kV) is changed for a particular DRI setting, the average tube current (mAs) calculated automatically adjusts to maintain the same $CTDI_{Vol}$ calculated at the standard protocol of 120 kV [20].

2.4 Previous Studies on Auto kV

As automatic tube potential selection technology is a fairly recent development in computed tomography, and only two manufactures currently are implementing such a function, the past research on such technology is limited. First, two phantom based studies will be discussed followed by three previous patient based studies of interest. These studies will be discussed in an aim to convey what research has previously been done on automatic kV selection technology and what impacts were evident with the adjustment of the tube potential both on image quality and radiation dose.

The first study published in 2009 by Yu et al. aimed to provide a strategy for selecting tube potential for each individual patient that will optimize radiation dose and maintain image quality [25]. At the time of this study no automatic tube potential selection function had been available on CT systems, thus the motive behind the study. The strategy involved using an index of image quality, "iodine contrast to noise ratio with a noise constraint (iCNR_NC)" and a relative dose factor RDF. The RDF quantified the relative dose at each tube potential to achieve the image quality defined by the iCNR_NC. With this, a workflow was developed that automatically identified the optimal tube potential that was both dose efficient and possible based off of the patient size and diagnostic requirements. Researchers then carried out an experimental study using different sized semi anthropomorphic phantoms to demonstrate how the proposed strategy can be implemented and what impacts it had on radiation dose reduction with certain noise constraints. Across the various sized phantoms with each different noise constraint, there was a general decrease in radiation dose with the optimal tube potential selected. However, these dose reductions varied significantly, thus requiring further studies for validation of the results and methods [25].

In 2013 Schindera et al. published a study analyzing the effect of the Siemens' automatic tube potential selection function (CAREkV) on image quality and radiation in CT angiography using three difference sized phantoms [26]. This study utilized an aortic phantom filled with iodinated contrast, which was then place into three different water containers, simulating small, medium, and large sized patients. Each setup was scanned at the clinical standard protocol of 120 kV with ATCM (CARE Dose4D), and then with CARE Dose4D and CAREkV. The image noise was measured and recorded by taking the standard deviation of the signal in the aneurysmal thrombus. The CNR was calculated for the aorta using the same technique as described in equation 3 with the mean HU value of the aorta being 'A', mean HU value of aneurysmal thrombus as 'B', and SD being the noise value from the aneurysmal thrombus. With ^{CARE}kV implemented, 70 kV was automatically selected for the small, 80 kV was selected for the medium, and 120 kV was selected for the large water phantom. With the automatic tube potential selections the $CTDI_{Vol}$ was reduced by 55.3% for the small phantom, 48.9% for the medium phantom, and did not change for the large phantom in comparison to the standard protocol of 120 kV. The image noise increased by 75.2% and 74.7% at the lower tube voltages in the small and medium phantoms, respectively. The noise in the large phantom stayed constant. The CNR increased by 22.8% and 3.6% with CAREkV for the small and medium phantom sizes respectively, whereas the large phantom's CNR decreased by 2.3% [26]. As these first studies discussed were phantom based studies, the following studies are patient based studies that examined the image quality and radiation dose impact of CAREkV.

Published in 2014 was a study by Mayer et al. with the objective of evaluating the simultaneous use of automatic tube current modulation and automatic tube voltage selection (ATVS) for contrast enhanced chest and abdominal studies [27]. The primary focus was based on evaluating the image quality and radiation dose reduction impacts of the ATVS. Patients were split up into two groups depending on if they were scanned with a standard fixed tube current of 120 kV and ATCM (CARE Dose4D) or with Siemens ATVS (CARE kV) and ATCM enabled. Image quality parameters that were being compared between the two groups for statistical analysis were signal to noise ratio (SNR), contrast to noise ratio (CNR), and a subjective radiologist ranking of the image quality. A subjective radiologist image quality ranking gives insight to the clinical relevance or impact, but does not aid to future research repeatability making this parameter not as useful especially since no significant difference was seen between the two group's scores. The SNR and CNR were measured at various anatomical locations throughout the scan with ROIs placed within the liver, spleen, portal vein, abdominal aorta, psoas muscle, visceral fat, and air. The SNR was calculated with the same technique as described in section 2.1, while the CNR was calculated by dividing by the SD of the signal in the region of interest (A) instead of outside of the region of interest (B). It was found that the SNR had instances of both lower and higher values when comparing the two groups, but as expected with the functionality of Siemens CARE KV, CNR was maintained or improved in the group using the CARE kV vs. the standard fixed

120 kV. The liver CNR was significantly higher in the CAREkV group ($p = 0.0006$), whereas no significant difference in CNR was seen for the other organs. Furthermore, the SNR was significantly higher in the abdominal fat tissue of group B ($p < 0.0001$), whereas significantly lower SNR values were found in the liver parenchyma compared with group A ($p = 0.0003$). The dose indices compared were the $CTDI_{Vol}$ and DLP. The study stated, “For chest and abdomen CT, dose reductions of 16.8% and 18.4%, respectively, were observed compared with the ATCM alone.”[27].

Another study with a very similar approach as Mayer, et al. was published by Frellesen, et al. again with the purpose of investigating the influence of Siemen’s CAREkV in combination with their CARE Dose4D on image quality and exposure parameters on patients receiving contrast enhanced chest and abdominal CT scans [28]. The group with CARE Dose 4D and a fixed standard 120 kV were scanned on a 16 slice Siemens CT scanner, while the group with the CARE Dose 4D and CARE kV were scanned on a dual source 128 slice Siemens CT scanner. This study compared values of SNR, subjective radiologist image quality scores, $CTDI_{Vol}$ and DLP. It was reported that the SNR was consistently higher for the group without the CARE kV applied which makes sense with how the CARE kV technology is implemented to maintain CNR image values. The subjective radiologist scores showed slightly better scores with CARE kV & CARE Dose4D vs. 120 kV& CARE Dose4D. On a 1 to 5 scale with 1 being excellent the CARE kV group averaged a 1.34 score vs. the 1.41 score average of the fixed kV group. The exposure parameter results showed significant decrease with the application of CARE kV. There was a decrease of 33 and 35 percent in the $CTDI_{Vol}$ and DLP respectively when comparing the median values of the CARE kV group against the fixed

120kV group [28]. A major pitfall of this study was the use of two different CT scanners on the two groups of patients which affects the significance of the reported values. The newer CT scanner might have had other technological improvements that abetted the improved image quality and dose reduction.

May, et al. evaluated the image quality and dose reduction in head and neck contrast enhanced exams between groups scanned with ATCM at 120 kV and at 100kV [29]. It was reported that as expected, the SNR was higher for anatomical regions scanned at 120 kV vs. the 100 kV group, while CNR was higher for anatomical regions scanned at 100 kV vs. the 120 kV group. This study also used a subjective radiologist image quality scoring which conveyed no significant difference in scores between the 120 and 100 kV groups. The mean $CTDI_{Vol}$ for the 120 kV group was 12.5 mGy while the mean $CTDI_{Vol}$ for the 100 kV group was 11.5 mGy presenting a reduction in radiation dose indices.

The next section will describe the methods utilized for this study in an aim to understand the functionality of Toshiba's ^{SURE}kV technology. This will be done in an effort to create an understanding of adjusting tube potentials and the impact on image quality parameters and dose indices. It will also be of interest to keep in mind Siemen's CARE kV and the findings of the above studies to see what similarities or differences are evident between Siemen's and Toshiba's automatic tube voltage selection technology.

3. Methods

In order to evaluate the image quality variances that might arise with changing tube potential, a phantom study was conducted. All CT scans were performed at Oregon Health & Science University. The first scans were done on a Toshiba Aquilion ONE ViSION CT scanner located on the 8th floor Emergency Department of the University Hospital and the second set of scans were completed on a Philips Brilliance iCT located on the 9th floor of the Center for Health and Healing. The phantom studies were completed using two different sized attenuation rings and the ACR CT accreditation phantom (Gammex 464), resulting in three different phantom configurations. The ACR phantom has dimensions of 20 cm in the antero-posterior (AP) dimension and 20 cm in the lateral (LAT) dimension. The second phantom configuration consisted of the ACR phantom placed within a small attenuating ring (The Phantom Laboratory CTP 579-15) resulting in dimensions of 25 cm in the AP dimension and 35 cm in the LAT dimension. The third phantom configuration consisted of the ACR phantom placed with a large attenuating ring (The Phantom Laboratory CTP 651-15) with the subsequent dimensions of 30 cm in the AP dimension and 38 cm in the LAT dimension. The three different phantom configurations were utilized in order to simulate varying patient sizes. However, as the phantoms are uniform water equivalent material, a patient and the phantom configurations have distinct differences and thus, directly comparing a phantom to a patient would be unsuitable.

First, for scans on the Toshiba and Philips, just the ACR phantom was setup on the CT table “Head” first into the gantry and then aligned the phantom to the CT scanner’s alignment lasers as shown in Figure 11.

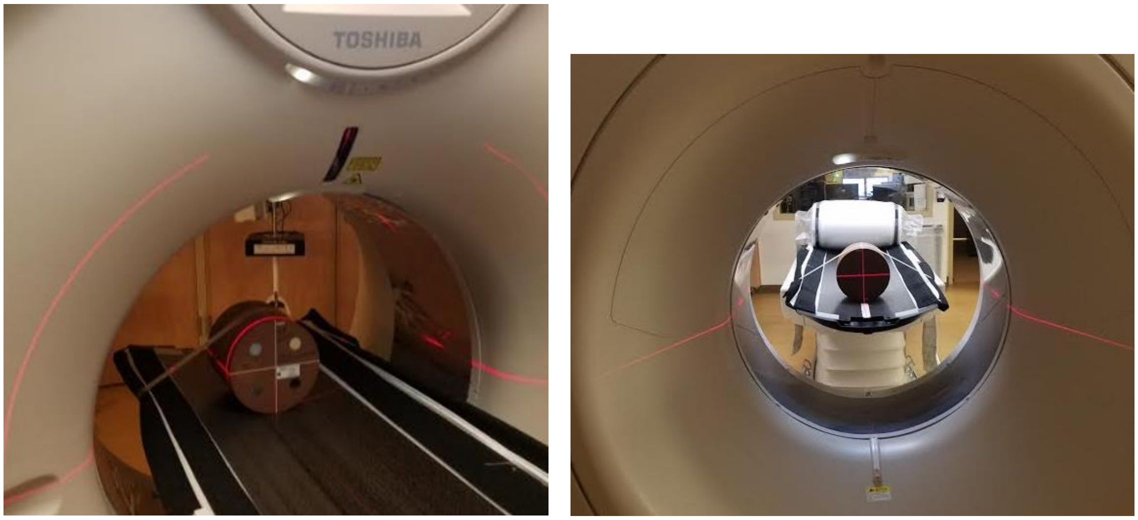

Figure 41: ACR Phantom Setup on the Toshiba Aquilion ONE ViSION

All the phantom setups were done in accordance with the ACR CT accreditation testing instructions [30].

For all three phantom configurations on the Toshiba Aquilion ONE ViSION and the Philips Brilliance iCT, the scan length was set at 16 cm. The FOV was set at 22 cm with just the ACR phantom, 28 cm with the small attenuation ring, and 30 cm with the large attenuation ring setup. The rotation time was set at the standard of 0.5 seconds on both systems unless a longer rotation time was necessary with the other scanning techniques set. The pitch was set at the reference standard for each system, 0.813 and 0.984 for the Toshiba and Philips scans respectively.

The target image quality on the Toshiba was set at the standard SD of 12.5. Other scan techniques that were held constant on the Toshiba Aquilion ONE ViSION include an image thickness of 5mm, SUREIQ settings (Body with standard SUREExposure 3D), and the reconstruction filter of FC 19 with AIDR 3D standard. AIDR 3D is Toshiba's Adaptive Iterative Dose Reduction (AIDR) algorithm that has three strength levels: mild, standard, and strong. Standard is the intermediate strength of the algorithm and is recommended for most clinical settings. The strength of the algorithm refers to the level of noise reduction through the amount of iterative reconstruction (mild has the least noise reduction and strongest has the greatest noise reduction) [11].

With all scans on the Philips Brilliance iCT, the target image quality level was set at the reference standard with a DRI of 23. A DRI of 23 corresponds to an effective mAs of 180 for the reference patient of 29 cm water equivalent diameter. The other scan techniques that were held constant include an image thickness of 5mm and iDose level 3 with the reconstruction filter B. Similar to Toshiba's AIDR 3D standard, Philips iDose level 3 just refers to the strength of their "Advanced Iterative Reconstruction Techniques" [31]. Philips iDose has levels 0 through 7, with the increasing strength (decreasing noise) correlating to the higher numbered level [31]. Specifically, iDose level 3 corresponds to 23% noise removal as state by Philips [31].

Both settings for the Toshiba and Philips scans are based on the recommended vendor settings found under the AAPM CT protocols for adult abdomen/pelvis CT scanning [32]. A summary table with each manufacturer's respective scan settings for this thesis is below.

	Toshiba	Philips
Detector Configuration	80 x .5 mm	64 x .625 mm
Scan Length	16 cm	16 cm
ATCM	^{SURE}Exposure3D	DoseRight
Target IQ Level	SD = 12.5	DRI = 23
Reconstruction	AIDR 3D	iDose
Iterative Reconstruction Strength	Standard	Level 3
Reconstruction slice thickness	5 mm	5mm

Table 1: Scan Parameters for Toshiba and Philips

3.1. ATCM

As ATCM is a standard feature in most clinical body CT protocol, the first set of scans applied the respective ATCM for Toshiba and Philips to the phantom configurations to examine the functionality and impact of such technology on CT image quality across various phantom sizes with changing tube potentials.

For all phantom configurations on the Toshiba scanner, a minimum mA was set at 10 with a maximum at 650. The ACR phantom was first scanned with ^{SURE}kV and ^{SURE}Exposure 3D enabled to see which tube potential was automatically selected by the system. With this same phantom setup and ^{SURE}Exposure 3D, the phantom was then scanned at the three other clinically available kVs that were not selected by the automatic kV selection function. As 120 kV is the clinical reference protocol, comparing the resulting data for the ^{SURE}kV protocol to the reference protocol was sought after. All scans were completed five times at each of the four kV's. The kV, maximum mA through the scan length, effective mAs, $CTDI_{Vol}$ and DLP were recorded for each scan from the system interface as shown in Figure 12.

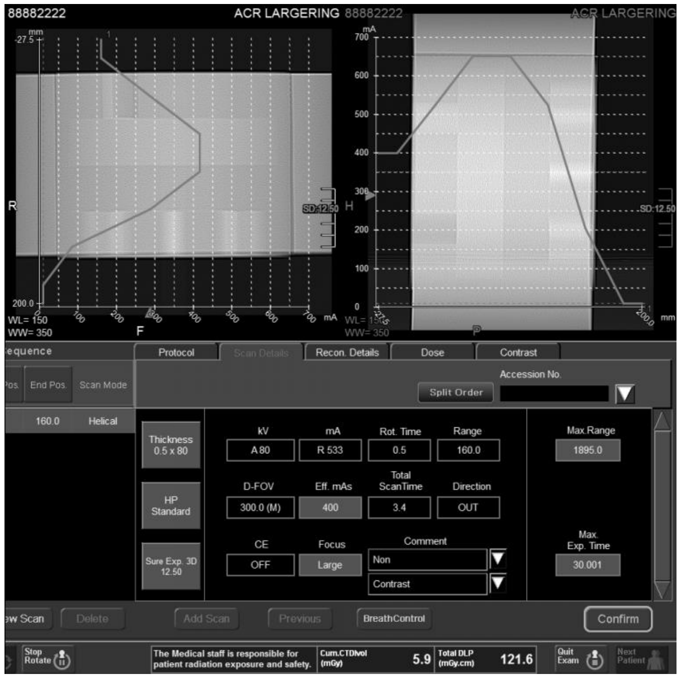

Figure 12: Toshiba CT Interface for Large Attenuation Ring Configuration

Next, for all three phantom configurations on the Philips scanner, a minimum mA was set at 10 with no maximum value set. As the Philips system does not have an automatic tube potential selection function, the ACR phantom was scanned at 80, 100, 120, and 140 kV with DoseRight enabled. All scans were completed five times at each of the four kV's. The kV, average effective mAs, average mA, minimum and maximum mA through the scan length, $CTDI_{Vol}$ and DLP were recorded for each scan from the system interface.

The processes described above for the Toshiba and Philips scans were repeated using the small and large attenuation ring configurations. Figure 13 shows the setup using the small attenuation ring on the Toshiba and the large attenuation ring on the Philips scanner.

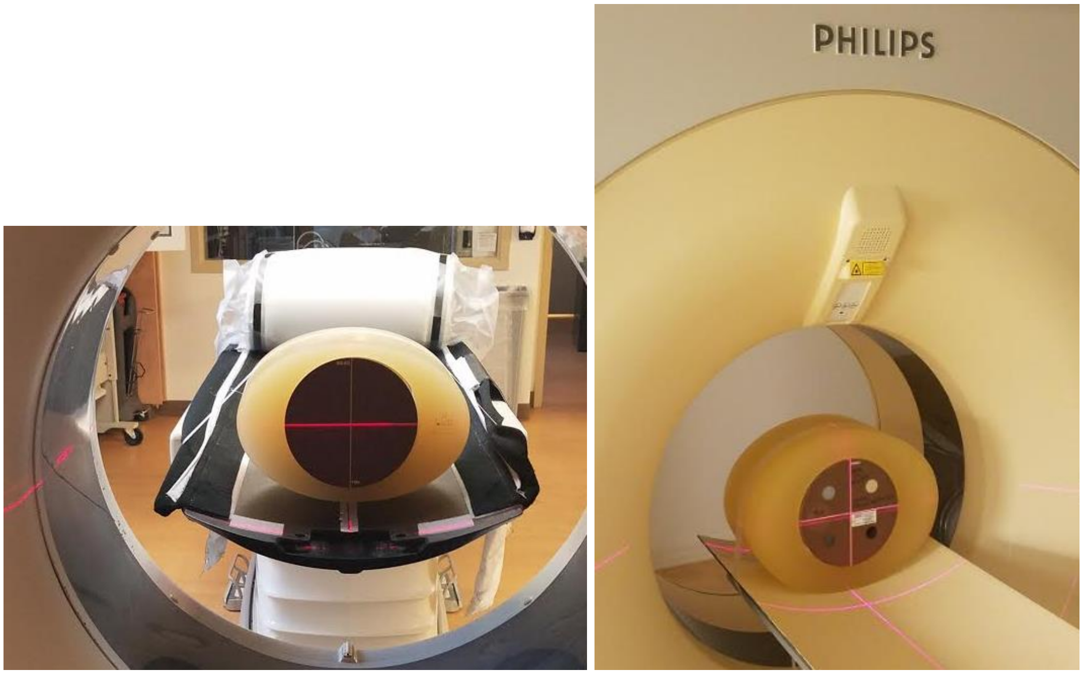

Figure 13: LEFT: Toshiba Small Attenuation Ring Setup

RIGHT: Philips Large Attenuation Ring Setup

3.2. Fixed $CTDI_{Vol}$

The next sets of scans were taken in an aim to see the clinical aspect of dose protocoling by fixing the $CTDI_{Vol}$ based on phantom size. These scans allow for analysis of the impacts on image quality metrics with changing tube potential and a fixed $CTDI_{Vol}$. The fixed $CTDI_{Vol}$'s of 10, 15, and 20 mGy were chosen to reflect varying dose levels that might be used for patients of varying sizes.

On the Toshiba scanner, each $CTDI_{Vol}$ target was obtained by adjusting the tube current to get as close as possible to the goal $CTDI_{Vol}$. Once the $CTDI_{Vol}$ was obtained, each phantom configuration was scanned once for each available kV. As was done previously, the kV, maximum mA, effective mAs, $CTDI_{VOL}$ and DLP were recorded for each scan from the system interface.

On the Philips scanner, adjustment of the effective mAs was necessary to meet each goal $CTDI_{Vol.}$ As was done on the Toshiba scanner, once the $CTDI_{Vol}$ was met, each phantom configuration was scanned once for each available kV and the relevant scan parameters and dose indices were recorded.

3.3. Fixed Tube Current

As the ACR CT accreditation phantom is being used for this thesis, it is pertinent to follow the ACR CT accreditation testing instructions when analyzing the data just as it would be for accreditation. The ACR CT accreditation testing instructions state that automatic mA modulation must be turned off and no automated dose reduction techniques may be used when scanning the phantom as part of ACR accreditation [30]. Following these instructions of scanning the ACR phantom with a fixed tube current, a fixed tube current was set at 300 mA for the Toshiba scans and 299 mA for the Philips scans. Each of the three phantom configurations was scanned once at each of the four clinically available tube potentials. The kV, $CTDI_{Vol}$, and DLP were then recorded for each scan.

3.4. Reading of the CT Scans

All of the CT scans were burned to discs and were read with RadiAnt DICOM viewer software. Each scan of the ACR phantom was examined to determine the image noise, CNR, and CT number accuracy. Analysis of the CT images was done following ACR CT accreditation instructions [30].

Module 1 of the ACR phantom is used to ensure positioning accuracy and CT number accuracy, but was only used for CT number accuracy for this research. The background material of Module 1 is water equivalent. To ensure correct setup and positioning, the module has steel BBs on the phantom surface at 3, 6, 9, and 12 o'clock positions. All four BBS need to be visible with the image slice for accurate positioning. To assess the CT number accuracy, there are cylinders of different materials: bone, polyethylene, water equivalent material, acrylic and air [30]. Figure 14 shows the list of acceptable HU values for each material when scanned at 120 kV.

Polyethylene HU between -107 and -84
Water HU between -7 and +7
Acrylic HU between +110 and +135
Bone HU between 850 and 970
Air HU between -1005 and -970

Figure 145: ACR CT Number Calibration Criteria [20]

The image read within module 1 of each scan, was the image slice with all four positional BBs visible as shown in Figure 15. Once the correct slice was determined, four ROI's of 200 mm^2 were placed within each cylinder as shown in Figure 15. The fifth ROI that was to be placed in the water equivalent region was placed based off the coordinates to ensure consistency across scans where the image is difficult to see. The mean value of each ROI was recorded according to the respective material they were located in.

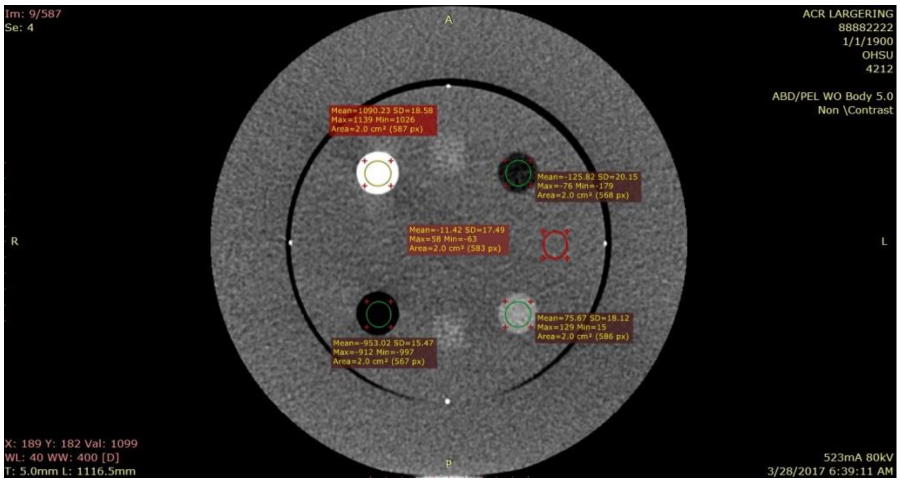

Figure 15: ACR Phantom Module 1 (Toshiba Large Attenuation Ring at 80 kV + ATCM)

Module 2 of the ACR phantom is used to assess the low contrast resolution and has a 25mm diameter cylinder which aids in assessing the CNR of an image slice. Because of the high noise level in the image, that is apparent in Figure 16, the location of the large cylinder had to be determined using the fixed tube current scans. Using the known coordinates from these scans, all other scans with the same phantom setup used the coordinates for consistency in placement of the 100 mm^2 ROIs. To calculate the CNR, subtract the mean signal in the higher ROI (A) that is on the large cylinder, from the mean signal in ROI outside the large cylinder (B) and then divide by the standard deviation of the signal in ROI (B) [30]. CNR: |A-B| / SD (B) (Equation 3 from section 2.1).

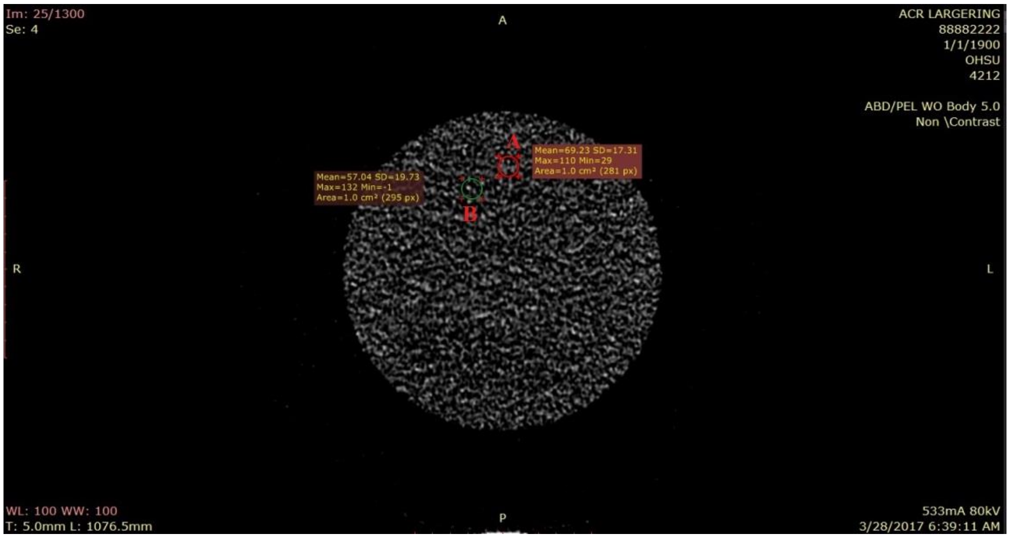

Figure 16: ACR Phantom Module 3 (Toshiba Large attenuation ring at 80 kV + ATCM)

Module 3 of the ACR phantom consists of a uniform tissue equivalent material and was used to determine the noise of the image data sets [30]. The window (WW) was set at 0 and level (WL) at 100 on the data slice where the two BBs were most visible A region of interest with an area of as close to 5000 mm^2 was to the right of the middle BB as shown in Figure 17. The standard deviation of the ROI is equal to the reported noise value.

$$\text{Noise} = SD\ of\ ROI \qquad (9)$$

This same approach was used on every image slice analyzed for every phantom configuration and scan settings.

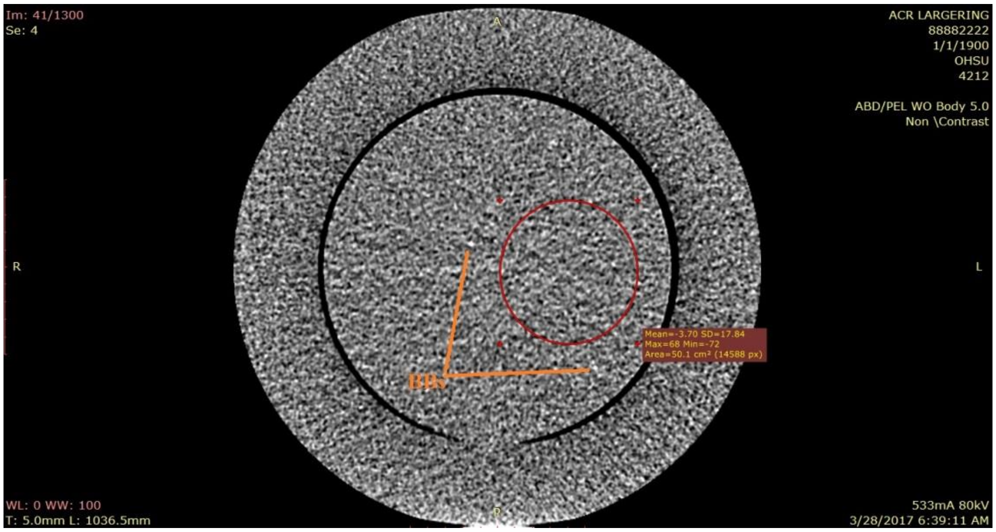

Figure 17: ACR Phantom Module 3 (Toshiba Large attenuation Ring at 80 kV + ATCM)

Statistical analysis was performed on the ATCM scans for both the Toshiba and Philips scans, comparing the CNR values at varying tube potentials. A one tailed paired t-test was performed between paired data sets of different tube potentials for each phantom configuration. A one tailed t-test was chosen in an aim to detect a directional difference between the CNR values with one being higher and one lower. By doing these tests, a p-value was obtained, giving a degree of significance to the effect of a changing tube potential on CNR.

The resulting data obtained from following the methodology described above provides data in relation to a commonly used CT protocol, such as the application of ATCM, and dose protocoling by fixing a CTDI for a certain exam type on a specific sized patient. The third scan parameter of fixing the tube current allows analysis of image quality based on the ACR Accreditation Phantom testing instructions. The entirety of this data is reported and discussed in the upcoming sections.

4. Results

4.1. ATCM

Tables 2 through 4 represent the data recorded for the section of this research that applied Toshiba's ATCM (^{SURE}Exposure 3D) with ^{SURE}kV and the other clinically available kV's that were not selected by the auto kV function. With each phantom configuration, 80 kV was automatically selected with ^{SURE}kV implemented and this is denoted in each table. The other clinically available kV's of 100, 120, 135 were then selected keeping the Target Image Quality, scan range, DFOV, pitch , rotation time, and max and min mA constant. Five scans were completed at each kV and the mean and standard deviation of the image quality metrics are displayed in Table 2 through 4 for their respective phantom configuration. The $CTDI_{Vol}$ at ^{SURE}kV's selected 80 kV is lower than the $CTDI_{Vol}$ at the standard protocol of 120 kV for just the ACR phantom setup, while small and large attenuation ring setups showed a $CTDI_{Vol}$ that is higher at ^{SURE}kV's selected 80 kV compared to 120 kV. The change in $CTDI_{Vol}$ from 120 kV to 80 kV for the ACR phantom, small attenuation ring, and large attenuation ring is 1.4 to 1.2 mGy, 2.9 to 3.6, and 3.9 to 5.9, respectively. The three phantom configurations resulted in an increase in CNR of 17.6% (p=0.05), 4.2% (p=0.41), 3.2% (p=0.38) for the ACR only, small, and large attenuation ring configurations respectively at the ^{SURE}kV selected 80 kV compared to the reference clinical protocol at 120 kV.

Table 2: Toshiba ACR Phantom Only Scans

ACR Only		Scan Time	3.4 seconds	Small Focal Spot			
Image Quality Level		Scan Range	DFOV (S Filter)	Pitch	Rotation Time	Max mA	Min mA
Standard (SD = 12.5)		16cm	22 cm	0.813	.5 sec	650 mA	10
		Scan Techniques					
kV	Max mA	Eff. mAs	$CTDI_{VOL}$	SSDE		Noise	CNR
80 ^{SURE}kV	105	73	1.2	2.16	**Average**	**12.84**	**0.52**
					$SD_{DAtA\ SET}$	**0.16**	**0.11**
100	60	36	1.4	2.52	**Average**	**10.53**	**0.70**
					$SD_{DAtA\ SET}$	**0.14**	**0.10**
120	35	21	1.4	2.52	**Average**	**12.99**	**0.44**
					$SD_{DAtA\ SET}$	**0.13**	**0.08**
135	25	15	1.4	2.52	**Average**	**11.57**	**0.63**
					$SD_{DAtA\ SET}$	**0.16**	**0.14**

Table 3: Toshiba ACR + Small Ring Scans

ACR + Small Ring		Scan Time	3.4 Seconds	Small FS for 100, 120, 135 kV. LG for 80 kV			
Image Quality Level		Scan Range	DFOV (M Filter)	Pitch	Rotation Time	Max mA	Min mA
Standard (SD = 12.5)		16cm	28 cm	0.813	.5 sec	650 mA	10
		Scan Techniques					
kV	Max mA	Eff. mAs	$CTDI_{VOL}$	SSDE		Noise	CNR
80 ^{SURE}kV	360	295	3.6	4.5	**Average**	**16.10**	**0.45**
					$SD_{DAtA\ SET}$	**0.23**	**0.18**
100	151	135	2.6	3.25	**Average**	**12.77**	**0.44**
					$SD_{DAtA\ SET}$	**0.23**	**0.05**
120	100	73	2.9	3.625	**Average**	**13.02**	**0.43**
					$SD_{DAtA\ SET}$	**0.16**	**0.02**
135	85	55	3.2	4	**Average**	**13.01**	**0.47**
					$SD_{DAtA\ SET}$	**0.21**	**0.12**

Table 4: Toshiba ACR + Large Ring Scans

ACR + Large Ring		Scan Time	3.4 seconds	Small FS for 100, 120, 135 kV. LG for 80 kV			
Image Quality Level		Scan Range	DFOV (M Filter)	Pitch	Rotation Time	Max mA	Min mA
Standard (SD = 12.5)		16cm	30 cm	0.813	.5 sec	650 mA	10
		Scan Techniques					
kV	Max mA	Eff. mAs	$CTDI_{VOL}$	SSDE		Noise	CNR
80 ^{SURE}kV	530	400	5.9	6.372	**Average**	**17.91**	**0.47**
					$SD_{DAtA\ SET}$	**0.06**	**0.12**
100	255	227	4.5	4.86	**Average**	**13.43**	**0.46**
					$SD_{DAtA\ SET}$	**0.21**	**0.14**
120	140	123	3.9	4.212	**Average**	**14.34**	**0.46**
					$SD_{DAtA\ SET}$	**0.20**	**0.07**
135	116	92	4.2	4.536	**Average**	**14.58**	**0.44**
					$SD_{DAtA\ SET}$	**0.17**	**0.10**

Tables 5 through 7 present the data recorded for the section of this research that applied Philip's ATCM (DoseRight) with the clinically available kVs. Throughout the scans of the different phantom configurations, the DoseRight Index, scan range, FOV, and min mA were kept constant. With the small attenuation ring configuration at 80 kV it was necessary to increase the rotation time to 1 second because the system was hitting a tube limit with a rotation time of 0.5 seconds. To also avoid tube limits with the large attenuation ring setup, at 80 kV the rotation time was changed to 1 second with a pitch of .608, and at 100 kV the pitch was changed to 0.75 seconds. Five scans were completed at each kV and the mean and standard deviation of the image quality metrics are displayed in Table 5 through 7 for their respective phantom configuration. As with the Toshiba data, the $CTDI_{Vol}$ at 80 kV is lower than the $CTDI_{Vol}$ at the standard protocol of 120 kV for just the ACR phantom setup, while small and large attenuation ring setups rsulted in higher $CTDI_{Vol}$ at 80 kV compared to 120 kV. The change in $CTDI_{Vol}$ from 120 kV to 80 kV for the ACR phantom, small attenuation ring, and large attenuation ring is 6.6 to 6.2 mGy, 14.7 to 14.9, and 24 to 26.2, respectively. In contrast to the Toshiba scans, the three phantom configurations on the Philips with ATCM resulted in a decrease in CNR of 12.6% (p=0.02), 14.7% (p=0.20), 16.1% (p=0.01) for the ACR phantom, small, and large attenuation ring configurations respectively at 80 kV compared to the reference clinical protocol at 120 kV. Comparing the three phantom configurations scanned at 100 kV against those at 120 kV a higher CNR was observed at 100 kV for the ACR phantom only and the small attenuation ring by 3.7% (p= 0.09) and 3.5% (p=0.35). The CNR was lower at 100 kV compared to 120 kV with the large attenuation ring by 25% (p= 0.01).

Table 5: Philips ACR Phantom Only Scans

ACR ONLY		Scan Time		2.9					
Target Image Quality Level DRI =23		Scan Range 16cm		FOV 30 cm	Pitch 0.984	Rotation Time .5 sec		Max mA —	Min mA 10
Scan Techniques									
kV	Average Eff. mAs	Averge mA	min mAs	max mAs	$CTDI_{VOL}$	SSDE		Noise	CNR
80	291	573	220	326	6.2	11.16	**Average**	**6.19**	**0.78**
							$SD_{DATA\ SET}$	**0.27**	**0.06**
100	146	288	110	164	6.4	11.52	**Average**	**5.77**	**0.93**
							$SD_{DATA\ SET}$	**0.26**	**0.02**
120	90	178	69	100	6.6	11.88	**Average**	**5.49**	**0.89**
							$SD_{DATA\ SET}$	**0.09**	**0.03**
140	62	124	49	70	6.8	12.24	**Average**	**5.56**	**0.95**
							$SD_{DATA\ SET}$	**0.13**	**0.06**

Table 6: Philips ACR + Small Ring Scans

ACR + Small Ring		Scan Time		2.9					
Target Image Quality Level DRI =23		Scan Range 16cm		FOV 30 cm	Pitch 0.984	Rotation Time .5 sec		Max mA —	Min mA 10
Scan Techniques									
kV	Average Eff. mAs	Averge mA	min mAs	max mAs	$CTDI_{VOL}$	SSDE		Noise	CNR
80	705	6954	433	796	14.9	18.625	**Average**	**10.24**	**0.52**
Rotation time	1						**$SD_{DATA\ SET}$**	**0.44**	**0.16**
100	338	667	221	378	14.9	18.625	**Average**	**9.59**	**0.63**
							$SD_{DATA\ SET}$	**0.71**	**0.11**
120	201	396	129	224	14.7	18.375	**Average**	**9.18**	**0.61**
							$SD_{DATA\ SET}$	**0.61**	**0.11**
140	135	266	88	150	14.6	18.25	**Average**	**9.16**	**0.55**
							$SD_{DATA\ SET}$	**0.52**	**0.07**

Table 7: Philips ACR + Large Ring Scans

ACR + Large Ring		Scan Time		2.9					
Target Image Quality Level DRI =23		Scan Range 16cm		FOV 30 cm	Pitch 0.984	Rotation Time .5 sec		Max mA —	Min mA 10
Scan Techniques									
kV	Average Eff. mAs	Averge mA	min mAs	max mAs	$CTDI_{VOL}$	SSDE		Noise	CNR
80	1236	752	881	1371	26.2	28.296	**Average**	**11.81**	**0.51**
Rotation time 1	Pitch .608						**$SD_{DATA\ SET}$**	**0.20**	**0.08**
100	560	736	343	630	24.6	26.568	**Average**	**11.17**	**0.45**
Rotation Time	0.75						**$SD_{DATA\ SET}$**	**0.30**	**0.07**
120	328	646	207	367	24	25.92	**Average**	**10.54**	**0.60**
							$SD_{DATA\ SET}$	**0.34**	**0.08**
140	215	425	137	241	23.4	25.272	**Average**	**11.21**	**0.49**
							$SD_{DATA\ SET}$	**0.55**	**0.05**

4.2. Fixed $CTDI_{Vol}$

Tables 8 and 9 show the data recorded for Toshiba and Philips scans respectively for the section of this research that applied a constant $CTDI_{Vol}$ of 10 mGy to represent a small size adult patient dose index. One scan of the ACR Accreditation phantom with no attenuation rings was done at each clinically available kV. The tube potential of 80 kV required a rotation time of 1 second compared to 0.5 seconds for the other available kVs to achieve the goal of a10 mGy $CTDI_{Vol.}$ on both the Toshiba and Philips systems . The Image quality metrics were then recorded once the images were analyzed. The resulting CNR decreased with increasing tube potential for the Toshiba scans, while the Philips scans did not show any definite relationship.

Table 8: Toshiba ACR Phantom Only with a Fixed CTDI of 10 mGy

kV	Eff. mAs	Rotation Time	mA	CTDI	Noise	CNR
80	332	1.0 sec	270	10	6.94	1.08
100	178	.5 sec	290	10.1	6.68	0.91
120	110	.5 sec	180	10	8.06	0.86
135	86	.5 sec	140	10.2	7.25	0.85

Table 9: Philips ACR Phantom Only with a Fixed CTDI of 10 mGy

kV	Eff. mAs	Rotation Time	mA	CTDI	Noise	CNR
80	470	1	462	10	5.08	1.02
100	228	0.5	449	10	4.91	0.98
120	137	0.5	270	10	4.52	1.02
140	92	0.5	181	10	4.68	1.08

Tables 10 and 11 presents the data recorded for the Toshiba and Philips scans respectively that adjusted the tube current (Toshiba) or effective mAs (Philips) to maintain a constant $CTDI_{Vol}$ of 15 mGy. One scan of the ACR phantom and small attenuation ring was done at each clinically available kV. A rotation time of 1.5 seconds was required for the 80 kV scan on the Toshiba scanner and 1 second on the Philips scanner. All other scans were completed with a rotation time of 0.5 seconds for the other available kVs. The Image quality metrics were then recorded once the images were analyzed. As with the fixed $CTDI_{Vol}$ of 10 mGy and the ACR phantom only, the resulting CNR decreased with increasing tube potential for the Toshiba scans, while the Philips scans did not show any definite relationship.

Table 10: Toshiba ACR + Small Ring with Fixed CTDI of 15 mGy

kV	Eff. mAs	Rotation Time	mA	CTDI	Noise	CNR
80	590	1.5 sec	320	15.4	10.50	0.61
100	283	.5 sec	460	15.3	9.86	0.60
120	184	.5 sec	300	15.3	10.74	0.59
135	141	.5 sec	230	15.6	10.87	0.52

Table 11: Philips ACR + Small Ring with Fixed CTDI of 15 mGy

kV	Eff. mAs	Rotation Time	mA	CTDI	Noise	CNR
80	707	1	695	15	10.52	0.65
100	342	0.5	673	15	9.59	0.50
120	205	0.5	403	15	9.74	0.64
140	139	0.5	274	15	9.65	0.48

Tables 12 and 13show the data recorded for the Toshiba and Philips scans respectively that aimed to maintain a constant $CTDI_{Vol}$ of 20 mGy. . One scan of the ACR phantom and large attenuation ring was done at each clinically available kV. On the Toshiba and Philips scanners, a tube rotation time of 1 second was required at 80 kV to meet the requirement of a 20 mGy $CTDI_{Vol}$. All other scans were completed with a rotation time of 0.5 seconds for the other available kV's. The Image quality metrics were then recorded once the images were analyzed. Both the Toshiba and Philips data show a decrease in CNR with increasing kV.

Table 12: Toshiba ACR + Large Ring with Fixed CTDI of 20 mGy

kV	Eff. mAs	Rotation Time	mA	CTDI	Noise	CNR
80	726	1.0 sec	590	20	12.91	0.83
100	369	.5 sec	600	19.9	13.28	0.61
120	227	.5 sec	370	19.9	12.79	0.55
135	178	.5 sec	290	19.7	12.85	0.52

Table 13: Philips ACR + Large Ring with Fixed CTDI of 20 mGy

kV	Eff. mAs	Rotation Time	mA	CTDI	Noise	CNR
80	945	1	902	20	15.46	0.61
100	455	0.5	895	20	12.49	0.52
120	273	0.5	537	20	13.00	0.51
140	185	0.5	364	20	12.09	0.44

4.3. Fixed Tube Current

The Toshiba and Philips data recorded with only the ACR phantom setup and a fixed tube current are displayed in Tables 14 and 15 correspondingly. The Toshiba scans had a fixed tube current of 300 mA and the Philips scans had a fixed tube current of 299 mA. All scans were done with a rotation time of .5 seconds and at all the clinically available kVs. The resultant $CTDI_{Vol}$ for each kV was recorded along with the image quality metrics once the images were analyzed. From 80 to 120 kV, the $CTDI_{Vol}$ increased by a factor of 3.02 for the Toshiba scans and increased by a factor of 3.47 for the Philips scans.

Table 14: Toshiba ACR Phantom Only with Fixed Tube Current of 300 mA

					CT # Accuracy				
kV	Rotation Time	CTDI	Noise	CNR	Poly	Water	Acrylic	Bone	Air
80	.5 sec	5.5	9.35	0.74	-129.24	-0.06	100.39	1253.84	-983.45
100	.5 sec	10.4	7.06	0.89	-107.53	0.56	115.22	1055.35	-984.91
120	.5 sec	16.6	5.99	0.93	-96.11	0.97	121.86	940.50	-984.26
135	.5 sec	22	5.34	1.01	-91.41	1.09	127.46	885.94	-984.03

Table 15: Philips ACR Phantom Only with Fixed Tube Current of 299 mA

kV	Rotation Time	CTDI	Noise	CNR	CT # Accuracy				
					Polyethylene	Water	Acrylic	Bone	Air
80	.5 sec	3.2	8.48	0.49	-122.53	1.20	110.42	1220.51	-997.32
100	.5 sec	6.7	6.06	0.93	-103.36	1.45	125.07	1019.78	-996.03
120	.5 sec	11.1	4.35	1.28	-90.02	2.96	132.72	903.70	-966.87
140	.5 sec	16.5	3.66	1.25	-83.30	3.26	137.17	830.44	-995.36

Tables 16 and 17 correspond to the Toshiba and Philips data recorded with the ACR phantom and small attenuation ring configuration and a fixed tube current. As mentioned previously, the Toshiba scans had a fixed tube current of 300 mA and the Philips scans had a fixed tube current of 299 mA. From 80 to 120 kV, the $CTDI_{Vol}$ increased by a factor of 3.19 for the Toshiba scans and increased by a factor of 3.47 for the Philips scans.

Table 16: Toshiba ACR + Small Ring and Fixed Tube current of 300 mA

kV	Rotation Time	CTDI	Noise	CNR
80	.5 sec	4.8	15.63	0.64
100	.5 sec	9.4	10.10	0.49
120	.5 sec	15.3	11.04	0.38
135	.5 sec	20.4	10.13	0.55

Table 17: Philips ACR + Small Ring and Fixed Tube current of 300 mA

kV	Rotation Time	CTDI	Noise	CNR
80	.5 sec	3.2	26.33	0.29
100	.5 sec	6.7	14.34	0.40
120	.5 sec	11.1	11.80	0.49
140	.5 sec	16.5	9.58	0.32

The data for the fixed tube current scans with the ACR phantom and the large attenuation ring for Toshiba and Philips are shown in Tables 18 and 19 in that order. Toshiba has a fixed tube current of 300 mA, while Philips fixed tube current was set at 299 mA. The $CTDI_{Vol}$ increased by the same factors for both Toshiba and Philips as they did with the small attenuation ring between 80 and 120 kV. Toshiba's $CTDI_{Vol}$ increased by a factor of 3.19 and Philips' $CTDI_{Vol}$ increase by a factor of 3.47.

Table 18: Toshiba ACR + Large Ring with Fixed tube current of 300 mA

kV	Rotation Time	CTDI	Noise	CNR
80	.5 sec	4.8	19.46	0.61
100	.5 sec	9.4	13.10	0.43
120	.5 sec	15.3	13.60	0.50
135	.5 sec	20.4	12.91	0.43

Table 19: Philips ACR + Large Ring with Fixed tube current of 300 mA

kV	Rotation Time	CTDI	Noise	CNR
80	.5 sec	3.2	38.15	0.20
100	.5 sec	6.7	21.70	0.46
120	.5 sec	11.1	15.21	0.61
140	.5 sec	16.5	13.02	0.50

5. Discussion

5.1 CT Number Accuracy

When examining the CT number accuracy of the scans, a common trend is quickly evident and this trend is well displayed below in Figure 18.

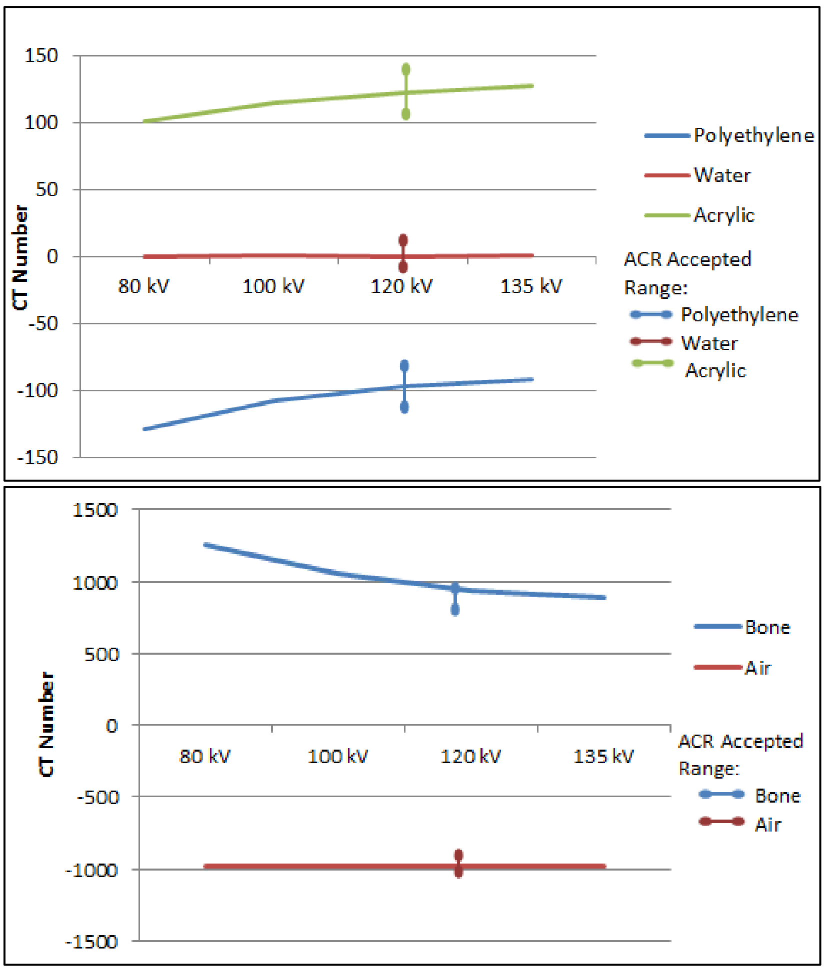

Figure 18: Toshiba CT # Trends (ACR Phantom ONLY with fixed tube current of 300 mA)

Very similar trend lines are apparent for all three configurations with ATCM applied, a fixed $CTDI_{Vol}$, and a fixed tube current of 300 mA on both the Toshiba and Philips scans. The fixed tube current data from the Toshiba scans is displayed in Figure 18 because it most accurately correlates to examining the accuracy of the CT numbers for these scans under the ACR Accreditation Testing Instructions. It is important to follow the directions as stated by the ACR Accreditation Testing Instructions to correctly compare the data to the ACR stated CT number calibration criteria given in Figure 14. These instructions state the setup of only the ACR phantom, and a clinical standard of 120 kV needs to be applied without the use of ATCM [30]. The range of acceptable values for each material is displayed at the clinical standard of 120 kV. The Toshiba ACR phantom only data at 120 kV and a fixed tube current of 300 mA, all fall within the acceptable range from the ACR instructions and differ from the published material CT number by: Polyethylene = -1.11, Water =0.97, Acrylic = 1.86, Bone = -14.5, Air = 14. 74. The Philips ACR phantom only data at 120 kV and a fixed tube current of 299 mA, all are within the ACR stated CT number calibration criteria except for the reported Air CT number. The acceptable range for air is -1005 HU to -970 HU while the air HU value was -966. The Overall variance from the published material's CT number was much greater for the Philips scans. The difference between the published and reported values for the Philips scans are as follows: Polyethylene= 4.98, Water= 2.96, Acrylic= 17.17, Bone=-51.3, Air= 33.93. The CT number trend for the Philips scan with the ACR phantom is shown in Figure 19 below.

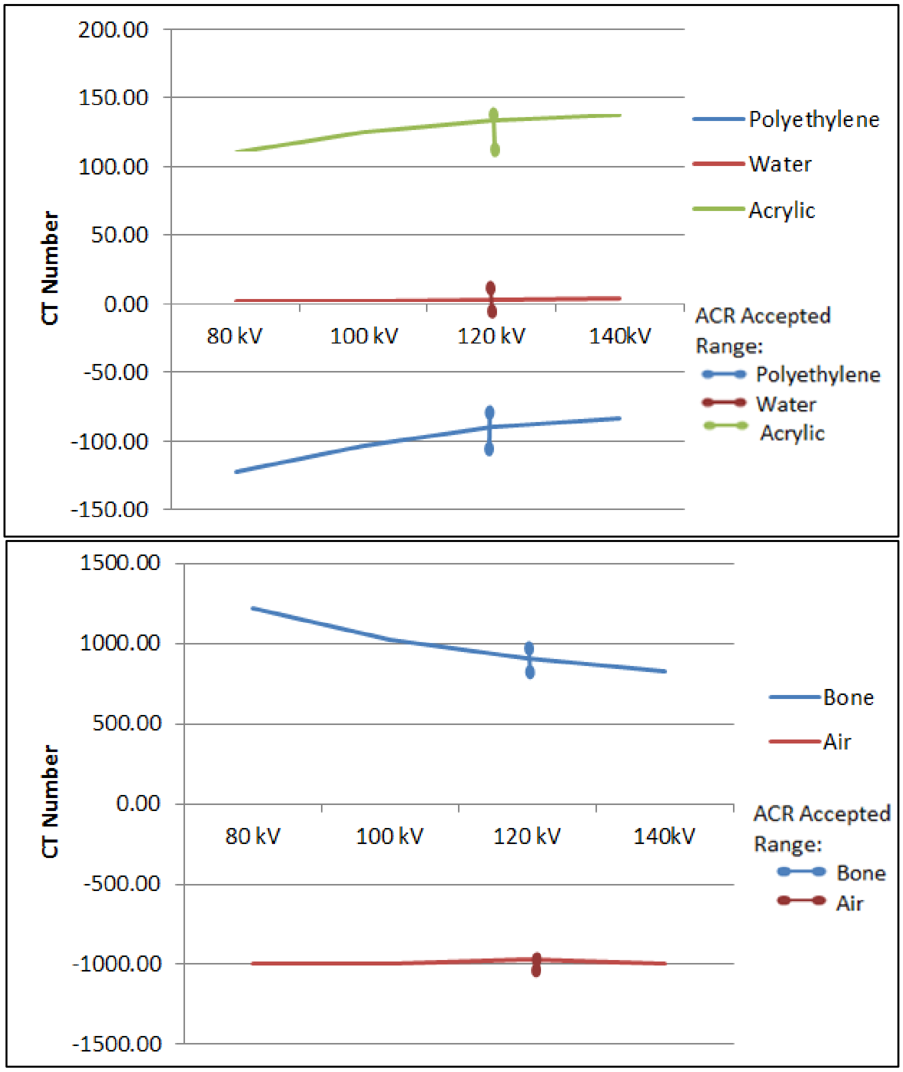

Figure 19: Philips CT # Trends (ACR Phantom ONLY with fixed tube current of 299 mA)

Understanding that the linear attenuation coefficient is dependent on the energy of interacting photons is important to understanding why the HU/CT number is changing as displayed in Figure 18 over the different kV's. Looking at the Polyethylene data from Table 14 for Toshiba shows the change of the CT number from -129.24 to -96.11 when going from 80 to 120 kV respectively. The relative increase in CT number from 80 to 120 kV (33.13 HU) means that relative to water; Acrylic is 3.313% more attenuating at the higher x-ray tube voltage [34]. The measured change in HU values from 80 to 120 kV results in a 26% change in HU. If this percentage change is calculated using the 80 and 120 kV HVL's of 4.08 mm and 6.06 mm respectively and National Institute of Standards and Technology (NIST) tables of attenuation coefficients, the change in HU values comes out to 29%, which is close to the measured percent change of 26%. Air and water HU values are fairly constant across tube potential and the reason being that the equation for HU values: $\mathrm{HU} = 1000\,\frac{\mu(object)-\mu(water)}{\mu(water)}$, is normalized to water (0 HU) and air (-1000 HU), thus the HU values are constant with changing kV's and that is displayed in Figure 18.

5.2 $\mathbf{CTDI_{Vol}}$

For a discussion on radiation dose indices and image quality metrics in CT, it should be recalled that relating the uniform phantom to a patient is incorrect. Thus, the results from the phantom configurations cannot be directly related to results that might be seen with patients.

The effect of automatic kV selection tools has been previously investigated and has been reported to reduce the radiation dose in patient studies [27,28,29]. However, when examining the phantom data for this thesis and comparing Toshiba's ^{SURE}kV automatically selected 80 kV $CTDI_{Vol}$ to the $CTDI_{Vol}$ at 120 kV, a decrease in radiation dose is not necessarily evident. Figure 20 below demonstrates the change in $CTDI_{Vol}$ with each phantom setup across the clinically available kVs.

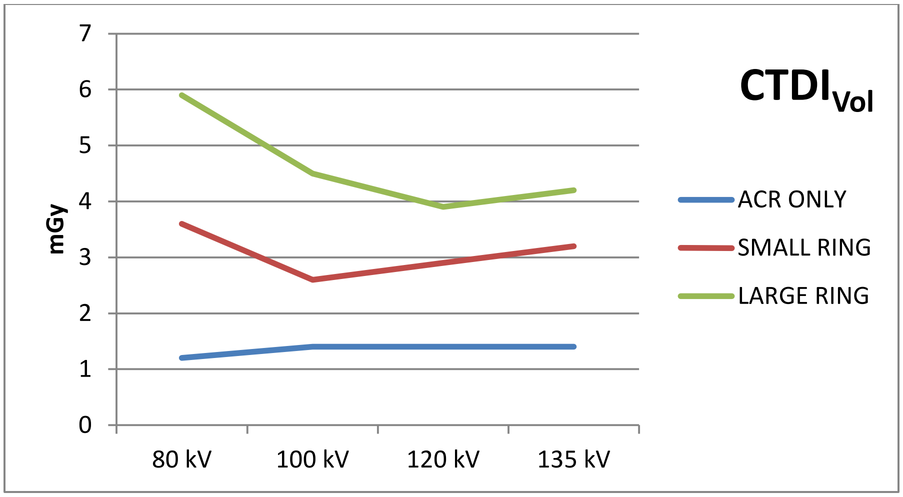

Figure 20: Toshiba CTDI$_{Vol}$ with ^{SURE}Exposure and clinically available kVs

With ^{SURE}kV applied, 80 kV was the tube potential that was automatically selected by the system for each phantom configuration. The ACR phantom alone was the only configuration that showed a decrease in CTDI$_{Vol}$ from the reference protocol of 120 kV to ^{SURE}kV's selection of 80 kV. This decrease was from 1.4 mGy to 1.2 mGy, equal to a 14.29% decrease. With the small attenuation ring setup, the CTDI$_{Vol}$ increased by 24.14% from 2.9 to 3.6 mGy, comparing the 120 kV protocol to the ^{SURE}kV selection of 80 kV. The large attenuation ring configuration resulted in an increase of the CTDI$_{Vol}$ of 51.28% (3.9 to 5.9) with the application of ^{SURE}kV and selection of 80 kV compared to the reference protocol. This increase in CTDI$_{Vol}$ could be due to ^{SURE}kV basing the selection of kV on the SD and maximum tube current possible, allowing the system to ramp of the tube current with a low kV, thus increasing the CTDI$_{Vol.}$

Even though Philips does not have an auto kV function, the system does aim to maintain image quality by keeping the CTDI$_{Vol}$ equal for the reference protocol of 120 kV when tube potential is changed. This is apparent in the data shown in Figure 21 where the CTDI$_{Vol}$s are fairly constant for each phantom configuration. Looking at the exact number shows similar results for the Philips scans as the Toshiba scans. The Philips scans with just the ACR phantom setup was the only scans to show a decrease in $CTDI_{Vol}$ from the reference protocol at 120 kV to 80 kV (6% decrease). The small and large attenuation ring setups reported 1.4% and 9.2% in increases respectively from 120 to 80 kV.

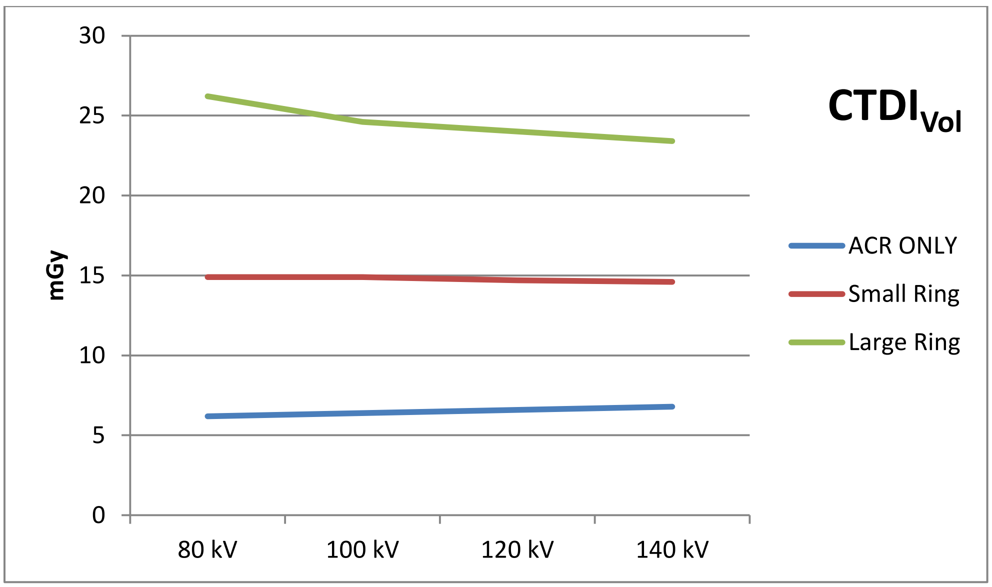

Figure 21: Philips $CTDI_{Vol}$ with DoseRight and clinically available kVs

These results differ from the Schindera et al. [26] phantom study that reported no increased in dose indices and reported decreases in $CTDI_{Vol}$ of 0 to 55.5% decrease with the auto kV function in use. Due to the varied effects on the exam $CTDI_{Vol}$ with a lower tube potential than the clinical reference protocol, no firm statement can be made about the impacts of implementing ^{SURE}kV on radiation dose reduction. It should also be noted that when looking at the values of the $CTDI_{Vol}$, the radiation dose delivered by the Philips system is much greater compared to that of the Toshiba scans with the ATCM employed

(6.6 mGy vs. 1.4 mGy for ACR only at 120 kV). These results could be in part due to how each particular vendor's ATCM functions in an attempt to maintain their own image quality reference and the slight differences in the slice thickness and detector rows for each scan parameters.

Taking into consideration the effective diameter of each phantom setup, and the respective factor from TG 204 [14] the SSDE was reported to get better estimation of the radiation dose from the Toshiba and Philips scans and is shown in Figures 22 and 23.

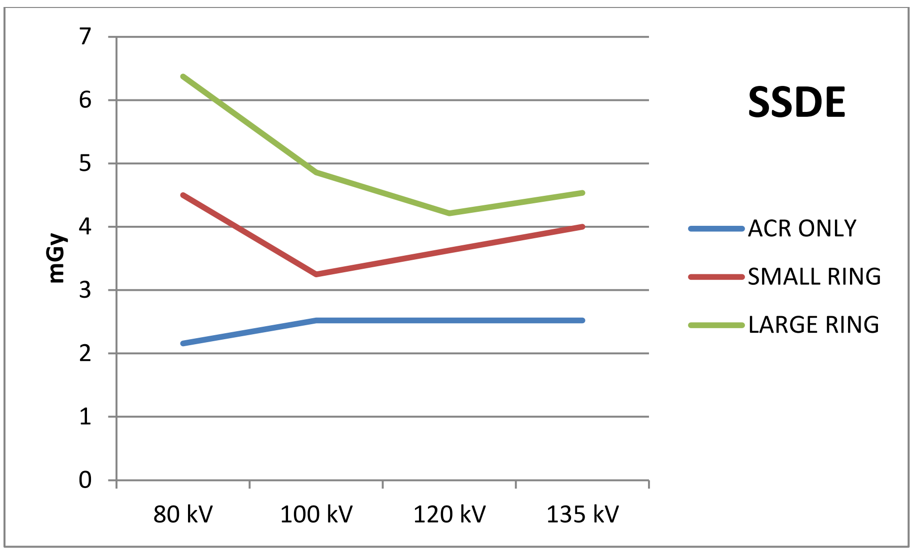

Figure 22: Toshiba SSDE with ^{SURE}Exposure and ^{SURE}kV

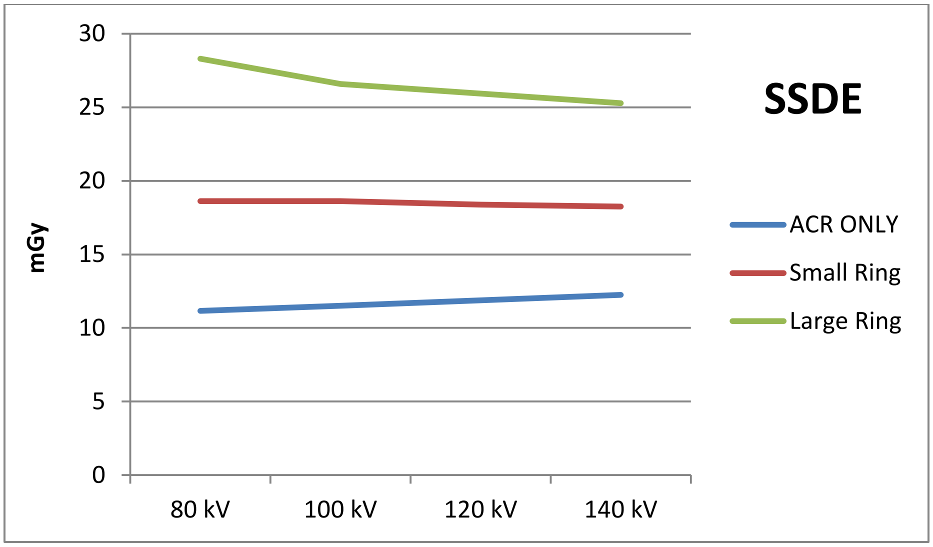

Figure 23: Philips SSDE with DoseRight

The smaller the effective diameter, the larger the multiplication factor reported in TG 204. This is because, with the smaller discrepancy from the center to peripheral (more uniform) dose used to calculate your $CTDI_W$ with the smaller effective diameter. The factor from TG 204 used to translate the $CTDI_{Vol}$ to the SSDE were 1.8, 1.25, and 1.08 for the ACR Only, small attenuation ring, and large attenuation rings setups respectively. Due to the larger factors being used to translate the $CTDI_{Vol}$ to SSDE with a smaller setup, a narrower range of values are evident between the three phantom configurations.

With the fixed tube current, the $CTDI_{Vol}$ across the three setups all increased linearly with an increasing kV as shown in Figure 24.

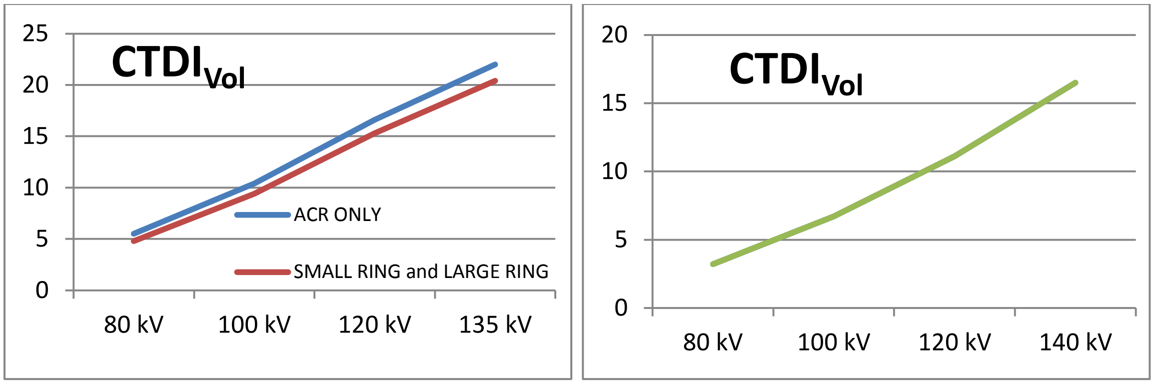

Figure 24: CTDI with fixed Tube Current of 300 mA vs. kV (LEFT: Toshiba, RIGHT: Philips)

The Toshiba scans with the small and large attenuation ring setup resulted in the same CTDI$_{Vol}$ for each available kV (2 lines on chart), while the CTDI$_{Vol}$ for the ACR only scans slightly higher. All the phantom configurations on the Philips resulted in the same CTDI$_{Vol}$ at each tube potential (thus only one line on chart). With these setups on the Toshiba, the CTDI$_{Vol}$ increased by a factor of 4.25 from 80 to 135 kV, while with the ACR phantom alone, the CTDI$_{Vol}$ increased by a factor of 4. The Philips scans all measured an increase by a factor of 5.16 in CTDI$_{Vol}$ from 80 to 140 kV. Interestingly, with nearly the same tube current, the Philips scans had a lower CTDI$_{Vol}$ at each tube potential available compared to the Toshiba scans. This is likely the result of the combination of the Philips scans having a lower pitch and the two systems having different beam filtration. In contrast, with each of Toshiba's and Philip's respective ATCM employed, Philips had a much higher radiation dose. The differing radiation doses with ATCM could be due to the different level and different type of image quality reference between Toshiba (SD=12.5) and Philips (DRI =23). Toshiba's ATCM algorithm is using a noise level in a water equivalent phantom, while Philip's ATCM algorithm is scaling the effective mAs for a given patient water equivalent diameter relative to their 29 cm water equivalent diameter reference patient.

Calculating the increase in x-ray tube output with equation 1, the value from 80 to 135 kV and 140 kV comes out to a factor of 2.85 and 3.06. These values are less than the measured increase in $CTDI_{Vol,}$ because $CTDI_{Vol}$ is dependent on the attenuation from the phantom and scatter from surrounding slices, thus it is not solely based on the relative tube output. The reported $CTDI_{Vol}$ percentage decrease from the reference protocol of 120 kV to 80 kV with a fixed tube current is 66.87% for just the ACR phantom and is 68.63% for the small and large attenuation ring set ups of the Toshiba scans. The Philips reported $CTDI_{Vol}$ percentage decrease from the reference protocol of 120 kV to 80 kV is 71.2%. These values are very close to the reported 68 % change mentioned prevoiusly for the change in $CTDI_{Vol}$ with changing kV using the 32 cm PMMA phantom.

5.3 Image Quality Metrics

In the 2013 phantom study by Schindera et al. using Siemens ATCM and auto kV function, the image noise (SD of ROI) increased by 75%, for both the small and medium sized phantoms at the lower tube potentials selected by the auto kV, while the large phantoms noise was constant due to the same tube potential (120 kV) being selected by the auto kV function [26]. As the radiation dose decreased with the lower kV selected by the auto kV function as discussed above, the noise increased with an inverse relationship. Patient based studies by May et al. and Frellesen et al. showed a similar trend with a lower SNR, which could be attributed to a higher noise level. These patient based studies also showed a lower radiation dose associating with the lower tube potential, thus the inverse relationship between noise and radiation dose.

Similarly to the Siemen's studies, the data collected for this thesis on the Toshiba Aquilion ONE ViSION CT scanner does show an increase in noise at the automatically selected kV compared to the noise at 120 kV. However, it does not display the same relationship between noise and dose. On the Toshiba scans, noise increased or decreased in coincidence with the radiation dose, not showing the inverse relationship between dose and noise as with the Siemens studies. ^{SURE}kV automatically selected 80 kV with each phantom configuration and just the ACR phantom was the only setup that had a decrease in $CTDI_{Vol}$ from 120 kV to the auto kV selected 80 kV. The noise decreased by 1.1% for just the ACR phantom setup, while the noise increased by 23.7% and 24.9% for the small and large attenuation phantoms respectively from 120 to 80 kV as shown in Figure 25.

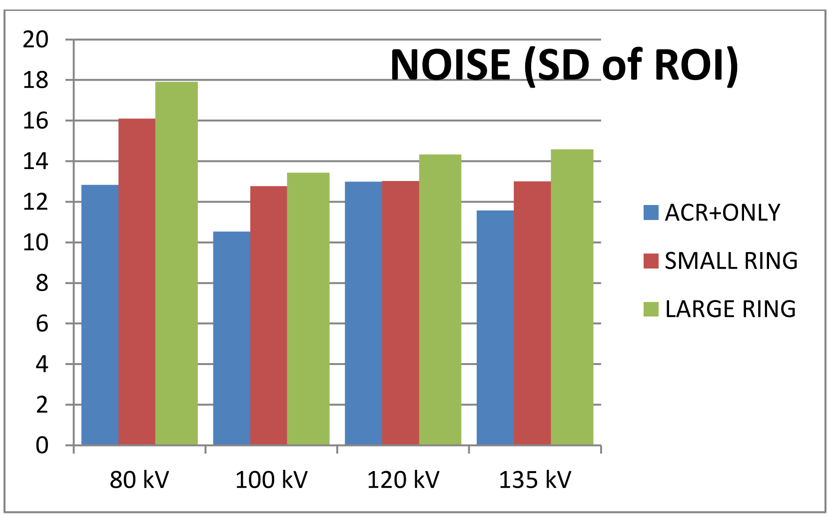

Figure 25: Toshiba Noise across tube Potentials with ATCM

The Philips scans followed the inverse relationship between radiation dose and noise with only the ACR phantom configuration. Just the ACR phantom setup resulted in a higher average noise at 80 kV and lower $CTDI_{Vol}$ when compared to the scans at 120 kV with DoseRight implemented. The other two phantom configurations resulted in higher noise and higher dose indices at the lower tube potential. The trend of the noise with different phantom configurations is shown in Figure 26 and illustrates a more consistent gradual decrease in noise with increasing tube potential when compared with Figure 25.

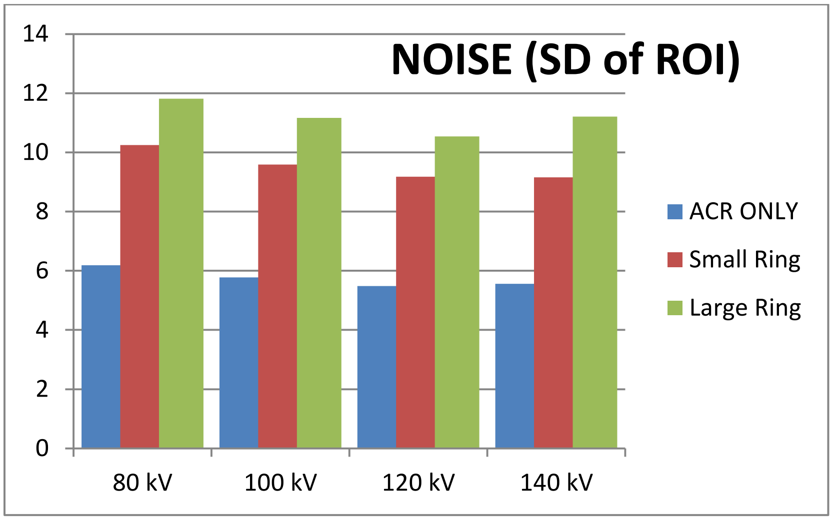

Figure 26: Philips Noise across tube Potentials with ATCM

The noise increased by 12.7%, 13.6%, and 12.0% for just the ACR phantom, small attenuation ring, and large attenuation ring respectively. The Philips scans also resulted in the trend of increasing noise with decreasing tube potential as was presented in the studies by May et al. and Frellesen et al. The Philips scans exhibited a higher average noise value at 80 kV than the reference protocol noise value at 120 kV across all phantom configurations with DoseRight implemented. This trend could be attributed to the fact that with a higher tube potential you are increasing the x-ray tube output and the penetrability of the x-rays, thus more photons penetrating the subject and then contributing to the image formation (decreasing noise).

When examining the noise values between the Toshiba scans and Philips with their respective ATCM, it is evident that the noise level for Toshiba's scans are higher. This relationship makes sense when looking back at the Toshiba scans with a much lower $CTDI_{Vol}$ compared to that of Philips with ATCM. The reason for these differences stems from the difference in functionality of each ATCM system respectively. Philips DoseRight has a starting ‘reference mAs’ according to the DRI level set that is scaled based on the subjects water equivalent diameter compared to that of their reference patient. In contrast, Toshiba’s ^{SURE}kV does not have a starting ‘reference mAs’ and is just increasing the mAs from zero to reach and maintain the set noise level. It is then evident that as Philips has a starting mAs value and Toshiba does not, the dose and noise would be higher and lower respectively for the Philips scans. The higher tube current/radiation dose relates to more photons projecting through the anatomy to the image detector, which results in less noise in the image. Comparing these systems solely based off of these phantom scans does pose some problems. Due to using low density water equivalent phantoms, the Toshiba system would see greater limitations in its functionality because it does not have a starting ‘reference mAs’ as does the Philips ATCM. In addition, there was no tube current modulation in the z-axis of the phantom further restricting the functionality of such technology.

The phantom study by Schindera et al. reported CNR values increasing by 22.8% and 3.6% for the small and medium phantom sizes respectively with the implementation of CAREkV, whereas the large phantom’s CNR decreased by 2.3% at the same tube potential [26]. The patient studies by Mayer et al., Frellesen et al., and May et al all reported higher CNR’s when CAREkV selected a lower tube potential than the reference standard of 120 kV.

The CNR relationship observed with the patient studies was confirmed by the Toshiba data that implemented ^{SURE}kV and ^{SURE}Exposure 3D with all three phantom configurations with the standard reference protocol of 120 kV and the ^{SURE}kV selected kV. As stated previously, ^{SURE}kV selected 80 kV with all three phantom configurations. Figure 27 displays the trend of the CNR across phantom setups and that the CNR is higher at the lower ^{SURE}kV selected tube potential.

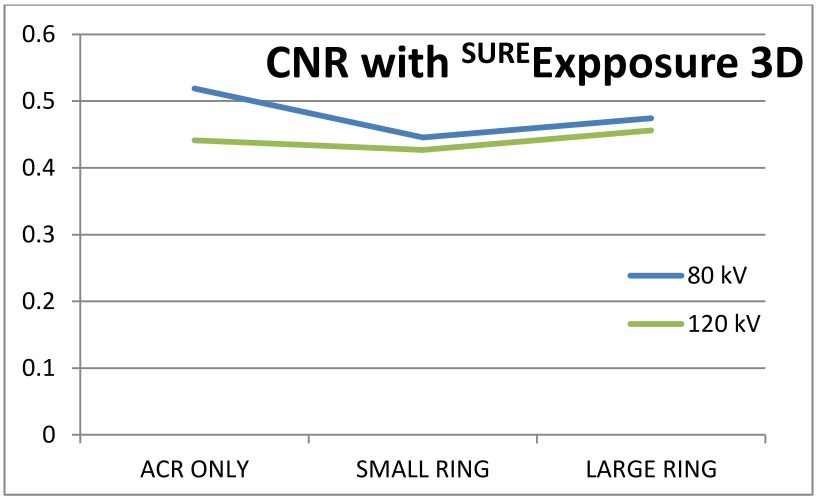

Figure 27: Toshiba CNR with ^{SURE}Exposure 3D

The CNR was 17.6% (p =0.05), 4.2% (p=0.41), 3.2% (p=0.38) higher for the ACR only, small, and large attenuation ring setups, respectively. With a confidence level of 90%, the only significant p-value was for the ACR only setup, which gives strong evidence that the CNR at 80 kV would be higher than at 120 kV with a larger population data set. As with the study by Schindera et al., the greatest increase in CNR was with the smallest phantom configuration and the least was with the largest phantom configuration. These results coincide with the fact that lowering the tube potential outputs a less penetrating spectrum that magnifies inherent differences in the attenuation coefficients between tissues, providing greater contrast in the diagnostic image. However, compared to the Schindera et al. study where there was a decrease in the dose indices with increasing CNR at 80 kV, the Toshiba scans with ^{SURE}kV showed increasing CNR with increasing $CTDI_{Vol}$ at 80 kV. This could be explained with how Siemens CAREkV in combination with the CARE Dose4D takes into account the $CTDI_{Vol}$ when optimizing the kV and mAs necessary to meet the needed image quality. Toshiba's ^{SURE}kV is not advertised to take into account the radiation dose when optimizing the tube current and potential, which is evident with the results.

With Philips not having an automatic kV function, the tube potential selection from Toshiba's ^{SURE}kV (80 kV) along with 100 kV was used to compare CNR's to the reference protocol of 120 kV. Varying from the Toshiba data from this thesis and Siemens data from previous studies, the Philips data displays a higher CNR at 120 kV than at 80 kV. The CNR was 12.6% (p=0.02), 14.7% (p=0.20), 16.1% (p=0.01) higher at 120 kV than 80 kV for the ACR only, small, and large attenuation ring arrangements in that order. The CNR was higher at 100 kV with the ACR phantom only and small attenuation ring by 3.7% (p= 0.09) and 3.5% (p=0.35) compared to at 120 kV. The CNR was lower at 100 kV compared to 120 kV with the large attenuation ring by 25% (p= 0.01). These trends can be seen in Figure in 28. The significant p-values reported above (< 0.1) at a confidence level of 90%, give strong evidence that the CNR differences between the respective tube potentials would be evident in a large data set.

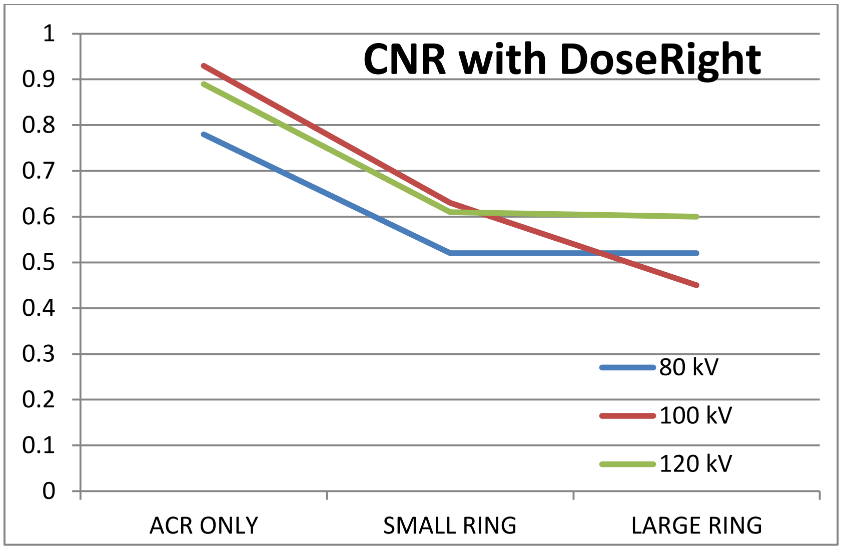

Figure 28: Philips CNR with DoseRight

It is also important to remember that all of the previous studies mentioned, make use of iodinated contrast, which will result in a much greater increase in CNR compared to this thesis data when tube potential is lowered. This is because when tube potential is lowered, the average x-ray energy is closer to the k-edge of iodine, creating greater differences in attenuation between the iodine and surrounding tissues.

When examining the CNR values between the tube current modulated scans of Philips and Toshiba, it is apparent the CNR values for the Philips modulated scans are higher in comparison to Toshiba ^{SURE}Exposure 3D scans. The reason for this could be because the mean contrast signal from the low contrast ROI for the Philips scans were higher at each tube potential then the Toshiba scans as is displayed in Figures 29 and 30 below. Along with the higher signal, the Philips scans had a lower noise level compared to the Toshiba scans as represented previously in Figures 25 and 26, which also contributes to the higher CNR values.

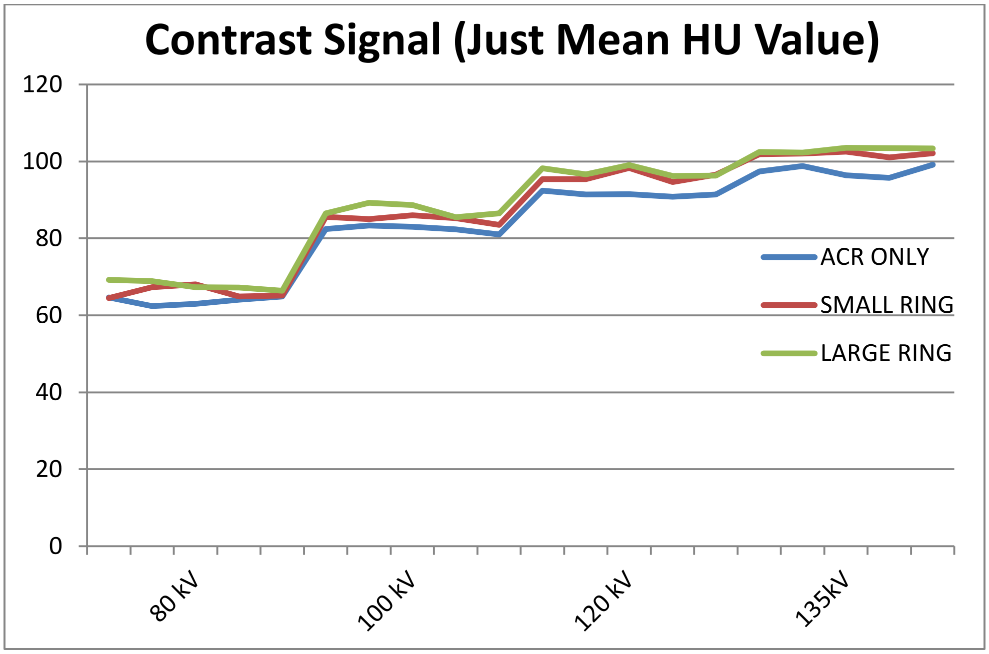

Figure 29: Mean HU value of Low Contrast ROI (Toshiba)

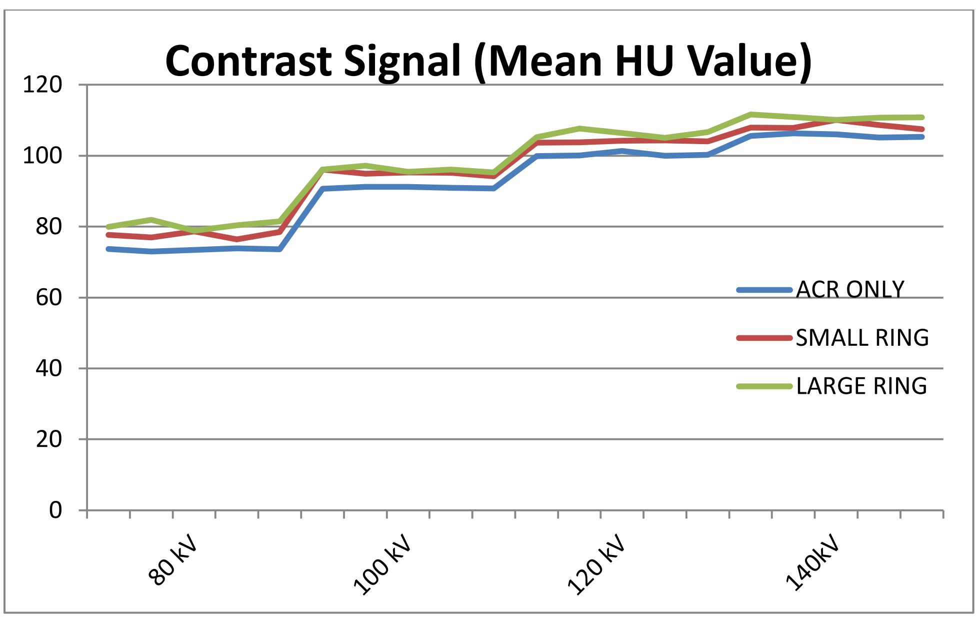

Figure 30: Mean HU value of Low Contrast ROI (Philips)

Next, aiming to see the impact of a fixed $CTDI_{Vol}$ across the available tube potentials by manipulating the tube current, allowed for analysis of another clinical technique such as dose protocoling. Each Toshiba phantom configuration with a fixed $CTDI_{Vol}$ displayed an increasing CNR with decreasing tube potential as shown in Figure 31. The fixed $CTDI_{Vol}$'s were 10, 15, and 20 mGy corresponding to the ACR phantom only, small attenuation ring, and large attenuation ring setups.

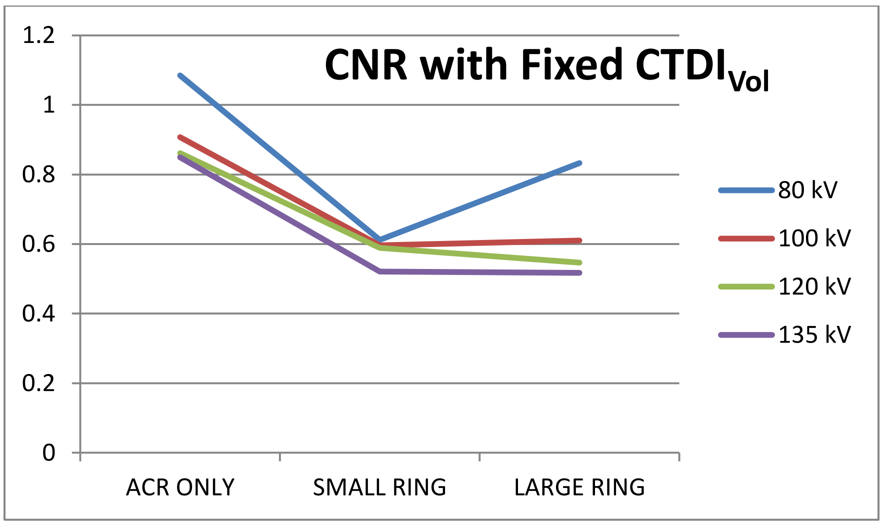

Figure 31: Toshiba CNR with a Fixed CTDI

In Figure 31 it is evident that the CNR at each phantom configuration is higher with a lower tube potential. This is to be expected as with each decrease of the tube potential, an increase of the subject contrast between materials is observed.

Comparatively, the Philips scans with the same fixed $CTDI_{Vol}$s as were used for the Toshiba scans, had different effects on the CNR with changing tube potentials. Figure 32 displays the relationship between tube potential and CNR for each phantom configuration.

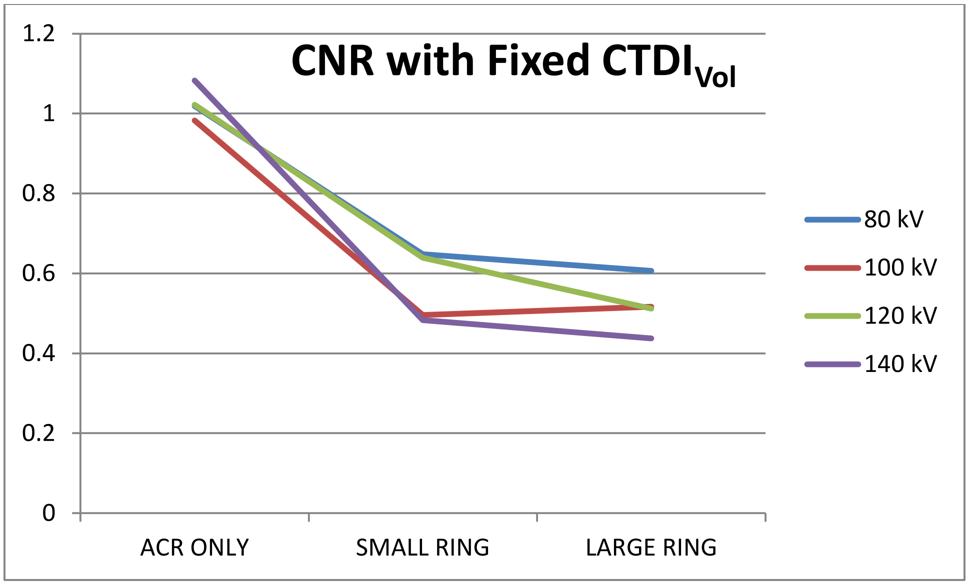

Figure 32: Philips Fixed CTDI CNR

As is evident, the large attenuation ring setup was the only configuration that resulted in the expected results of a higher CNR associating with the lower tube potential from 80 to 100 kV, 100 to 120 kV, and 120 to 140 kV. With just the ACR phantom configuration, the CNR was highest at 140 kV, then 120 kV, followed by 80 kV, and finally 100 kV. The difference of the highest and lowest CNRs with just the ACR phantom is only 0.10. With this small disparity, these unforeseen results could be due to the statistical variation of noise, which could produce the variation in CNRs reported.

6. Conclusions

A phantom study was carried out to assess the functionality of an automatic kV tool in combination with automatic tube current modulation. The impacts on image quality and radiation dose were explored in this study in an aim to see the possible clinical benefits and implementations of adjusting tube potential.

To start, a few limitations of current study need to be considered. First, this study was completed using a water equivalent phantoms which does not necessarily reflect the functionality of the two respective CT systems with clinical patients. Coinciding with this limitation is the fact that $^{\text{SURE}}$kV selected the lowest kV for all three different sized phantom setups, which does not reflect patient scans, as the phantom is of low density water equivalent material. Secondly, when comparing the Toshiba results against the Philips results it is not possible to know the exact differences between the iterative reconstruction algorithms of AIDR 3D and iDose. In addition, the strengths of each reconstruction technique are difficult to compare in part because AIDR 3D has three strength levels, whereas iDose has seven strength levels. Lastly, this study only used three phantom sizes that required the same tube current modulation over the z-axis for each scan, which does not represent the real world use of such technology clinically.

Considering some of these limitations, future possible studies are apparent. An in vivo patient study would be beneficial in examining the functionality of Toshiba's $^{\text{SURE}}$kV and seeing the interplay between the tube potential and tube current modulation across various patient anatomies. And, if a patient study was not possible, phantom studies utilizing configurations with greater effective diameters would be valuable to determine the thresholds of ^{SURE}kV's tube potential selection.

Based off of the data from this thesis a few conclusions can be drawn. While the implementation of Toshiba's ^{SURE}kV resulted in varied effects on radiation output, an improvement in image quality was evident for three phantom sizes when also using Toshiba's ATCM compared to the standard protocol of 120 kV. For the Philips scans with ATCM at the kV selected by Toshiba's ^{SURE}kV, no explicit improvement was seen in image quality across phantom configurations compared to the reference standard at 120kV.

However, it was evident that with each respective ATCM, Philips had a higher dose index and lower image noise compared to Toshiba at each tube potential and with each phantom configuration. It was mentioned previously and can be concluded that these differences stem from the difference in functionality of each ATCM. Philips DoseRight has a starting 'reference mAs' according to the DRI level set that is scaled based on the subjects water equivalent diameter compared to that of the Philips reference patient. Thus, Philips has a starting reference mAs no matter the size and density of subject/object. In contrast, Toshiba's ^{SURE}kV does not have a starting 'reference mAs' and simply increases the mAs to maintain the set noise level. Comparing these systems solely based off of these phantom scans does pose some problems. Due to using water equivalent phantoms, the Toshiba system would see greater limitations in its functionality compared to Philips as it does not have a starting 'reference mAs' as does the Philips ATCM.

In further analyzing Philips ATCM functionality, while the tube potential changed, the $CTDI_{Vol}$ stayed fairly constant for each phantom setup, confirming the expected functionality of DoseRight. It was also evident on the Toshiba CT scanner that with a fixed $CTDI_{Vol}$, an increase in CNR was possible when decreasing tube potential on all three different phantom configurations.

The entirety of this data does aid in furthering the understanding of the interplay between tube current, tube potential, and their impact on dose and image quality in CT. However, the results and conclusions provided should only be taken as results of a phantom study. The phantoms are uniform water equivalent material, thus having distinct differences from patients. This study is a starting point for future studies to provide greater clinically applicable data to CT exams, and provides important insight regarding the impact of tube current and tube potential on uniform water equivalent phantoms in CT.

Bibliography

[1] Gray, Joel E., Gary T. Barnes, and Michael J. Bronskill. The role of the clinical medical physicist in diagnostic radiology. No. 42. AAPM Report, 1994.

[2] Mettler Jr, Fred A., et al. "Radiologic and Nuclear Medicine Studies in the United States and Worldwide: Frequency, Radiation Dose, and Comparison with Other Radiation Sources—1950–2007 1." Radiology 253.2 (2009): 520-531.

[3] Angel, E. "Sure exposure: low dose diagnostic image quality." Tustin, CA: Toshiba America Medical Systems (2009).

[4] International Commission on Radiological Protection. Recommendations of the International Commission on Radiological Protection. Oxford, UK: Pergamon Press, 1977:ICRP publication no. 26

[5] May, Matthias S., et al. "Automated tube voltage adaptation in head and neck computed tomography between 120 and 100 kV: effects on image quality and radiation dose." Neuroradiology 56.9 (2014): 797-803.

[6] Europe, Toshiba Medical Systems. "Toshiba Medical Systems ANZ – SUREkV." Toshiba Medical Systems ANZ. Toshiba Medical Systems Europe, n.d. Web. 13 Apr. 2017. <http://www.toshiba-medical.eu/au/products/ct/sure-kv/>.

[7] RSNA/AAPM Physics Module, "CT Systems".

[8] Bushberg, Jerrold T., and John M. Boone. The essential physics of medical imaging. Chapter 10, "Computed Tomography". Lippincott Williams & Wilkins, 2011.

[9] "Computed Tomography (CT)." National Institutes of Health. U.S. Department of Health and Human Services, 02 Feb. 2017. Web. 06 Mar. 2017.

[10] "INTRODUCTION AND OVERVIEW." Interaction of Radiation with Matter. N.p., n.d. Web. 16 Apr. 2017. <http://www.sprawls.org/ppmi2/INTERACT/>.

[11] "Radiography Physics." N.p., n.d. Web. <https://www.nde-ed.org/EducationResources/CommunityCollege/Radiography/Physics/attenuationCoef.htm>.

[12] Nadrljanski, Mirjan M. "Computed tomography | Radiology Reference Article." Radiopaedia.org. N.p., n.d. Web. 05 Mar. 2017.

[13] RSNA/AAPM Physics Module, "CT Image Quality and Protocols".

[14] Boone, J. M., K. J. Strauss, and D. D. Cody. Size-specific dose estimates (SSDE) in pediatric and adult body CT examinations. No. 204. AAPM Report, 2011.

[15] Bushberg, Jerrold T., and John M. Boone. The essential physics of medical imaging. Chapter 11, “X-ray Dosimetry in Projection Imaging and Computed Tomography”. Lippincott Williams & Wilkins, 2011.

[16] RSNA/AAPM Physics Module, “Radiation Dose in CT”.

[17] McCollough, Cynthia H., et al. "CT dose index and patient dose: they are not the same thing." Radiology 259.2 (2011): 311-316.

[18] RSNA/AAPM Physics Module, “X-Ray Tubes and Spectra”.

[19] "CARE Dose4D CT Automatic Exposure Control System: Physics Principles and Practical Hints." Mayo Clinic, n.d. Web. 26 Feb. 2017.

[20] Philips. “Patient-centered CT imaging: New methods for patient-specific optimization1 of image quality and radiation dose”. 2012

[21] Dsct.editors@spiritlink.de. "CARE Dose 4D and Dose Curves." DSCT.com - your Dual-source CT experts. N.p., n.d. Web. 02 Mar. 2017.

[22] CARE Dose4D White Paper. Thomas Flohr, PhD Head of CT Physics and Applications. Siemenes Healthcare.

[23] Raman, Siva P., et al. "CT dose reduction applications: available tools on the latest generation of CT scanners." Journal of the American College of Radiology 10.1 (2013): 37-41.

[24] Angel, E. "AIDR 3D Iterative Reconstruction: Integrate, Automated, and Adaptive Dose Reduction.": Toshiba America Medical Systems (2012).

[25] Yu, Lifeng, et al. "Automatic selection of tube potential for radiation dose reduction in CT: a general strategy." Medical physics 37.1 (2010): 234-243

[26] Schindera, S. T., et al. "Effect of automatic tube voltage selection on image quality and radiation dose in abdominal CT angiography of various body sizes: a phantom study." Clinical radiology 68.2 (2013): e79-e86.

[27] Mayer, Caroline, et al. "Potential for radiation dose savings in abdominal and chest CT using automatic tube voltage selection in combination with automatic tube current modulation." American Journal of Roentgenology 203.2 (2014): 292-299.

[28] Frellesen, Claudia, et al. "Topogram-based automated selection of the tube potential and current in thoraco-abdominal trauma CT–a comparison to fixed kV with mAs modulation alone." European radiology 24.7 (2014): 1725-1734.

[29] May, Matthias S., et al. "Automated tube voltage adaptation in head and neck computed tomography between 120 and 100 kV: effects on image quality and radiation dose." Neuroradiology 56.9 (2014): 797-803.

[30] American College of Radiology, “CT Accreditation Program Testing Instructions”.

[31] iDose4 iterative reconstruction technique White Paper. Philips

[32] AAPM. Adult Routine Abdomen/Pelvis CT Protocols. (2015). http://www.aapm.org/pubs/CTProtocols/documents/AdultAbdomenPelvisCT.pdf

[33] National Raiology Data Registry. Exectuive Summary Report, July –Decemeber 2016. Dose Index Registry. Oregon Health & Science University.

[34] "CT Radiographic Techniques." CT Radiographic Techniques | Radiology | SUNY Upstate Medical University. N.p., n.d. Web. 22 April 2017. <http://www.upstate.edu/radiology/education/rsna/ct/technique.php>.